NUMERICAL SIMULATIONS AND ANALYSIS OF LAVA FLOW COOLING

Prepared for

U.S. Nuclear Regulatory Commission
Contract NRC–02–07–006

Prepared by

Debashis Basu[1]
Kaushik Das[1]
Stephen Self[2]

[1]Center for Nuclear Waste Regulatory Analyses
San Antonio, Texas

[2]U.S. Nuclear Regulatory Commission
Washington DC

March 2012

ABSTRACT

This report documents the results of a numerical analysis carried out to understand the cooling of lava flows in an external open environment using the computational fluid dynamics code/program ANSYS® FLUENT™ Version 12 (ANSYS, Inc., 2009). The Navier-Stokes equations are solved in two dimensions. A rectangular, tabular geometry for the lava body is considered. The lava and its surroundings are modeled as two-dimensional elements effectively forming three stacked layers. Movement of air (wind) is not modeled but is accommodated by keeping the ambient atmospheric temperature at 305 °K [89 °F]. The heat transfer between the top surface of the hot lava and the atmosphere is assumed to be controlled by the convective heat transfer and radiation. Simulations are conducted with different conditions and parameter sets: (i) lava cooling with constant viscosity, constant thermal conductivity, and constant density; (ii) lava cooling with constant viscosity, variable thermal conductivity, and variable density; (iii) lava cooling with variable viscosity, variable thermal conductivity and variable density; and (iv) lava cooling under the influence of rainfall. Simulations with constant properties are compared to those with variable properties. Transport of heat flow from the lava to its surroundings is modeled through radiation and convection from the surface as well as through conduction to the ground. Internally, a conduction-only approach moved heat from the interior outward. Simulation parameters for the lava properties are obtained from a previous numerical study on lava cooling after the 1997 Okmok (Alaska) eruption (Patrick, et al., 2004).

Computed results show that the lava temperature drops significantly and an upper crustal zone develops within the first few weeks of cooling. Simulations are carried out to represent a cooling period of 3 years; results show significant variation in the temperature over the whole computational period. The assumption of variable thermal conductivity and variable density along with constant viscosity results in plumelike thermal structures within the lava core region. However, in the simulations with variable viscosity, variable thermal conductivity, and variable density, small convection cells form in the core. Simulated results illustrate that the treatment of lava viscosity (constant or variable) in conjunction with other properties significantly influences the predicted temperature field.

The influence of rain on the lava cooling is also analyzed and is not noticeable during the initial time period (1 year). However, after a significant time (~2 years), the effect of rain is manifested through the lower values of the lava core temperature. The convective heat transfer coefficient seems to significantly influence the lava surface temperature. Convective heat loss dominates the heat transfer modes after the initial stages of radiative heat transfer, following the results of previous studies. Rates and cooling times similar to those found in previous modeled analyses of lava cooling are obtained by this alternative modeling approach.

REFERENCES

ANSYS, Inc. “ANSYS FLUENT Version 12.1, User’s Guide.” Canonsburg, Pennsylvania: ANSYS, Inc. 2009.

Patrick, M.R., J. Dehn, and K. Dean. “Numerical Modeling of Lava Flow Cooling Applied to the 1997 Okmok Eruption: Approach and Analysis.” *Journal of Geophysical Research.* Vol. 109. B03202, DOI: 10.1029/2003JB002537. 2004.

CONTENTS

FIGURES

FIGURES (continued)

TABLES

ACKNOWLEDGMENTS

This report describes work performed by the Center for Nuclear Waste Regulatory Analyses (CNWRA®) for the U.S. Nuclear Regulatory Commission (NRC) under Contract No. NRC–02–07–006. The activities reported here were performed on behalf of the NRC Office of Nuclear Material Safety and Safeguards, Division of Spent Fuel Alternative Strategies. This report is an independent product of CNWRA and does not necessarily reflect the view or regulatory position of NRC. The NRC staff views expressed herein are preliminary and do not constitute a final judgment or determination of the matters addressed or of the acceptability of any licensing action that may be under consideration at NRC.

The authors gratefully acknowledge D. Hooper for his technical review, E. Pearcy for his programmatic review, L. Mulverhill for her editorial review, and A. Ramos for his administrative support. M. Agarwal from ANSYS Company is also acknowledged for his advice and help in setting up the simulation cases used in this study. M. Muller helped with some of the figures.

QUALITY OF DATA, ANALYSES, AND CODE DEVELOPMENT

DATA: All CNWRA-generated original data contained in this report meet quality assurance requirements described in the Geosciences and Engineering Division Quality Assurance Manual. Sources of other data should be consulted for determining the level of quality of those data. The work presented in this report is documented in Scientific Notebook 825E (Das and Basu, 2011).

ANALYSES AND CODES: The general purpose computational fluid dynamics simulation code ANSYS® FLUENT™ Version 12.1 (ANSYS, Inc., 2009) was used to generate results for this report and is controlled in accordance with the CNWRA Technical Operating Procedure (TOP)–018, Development and Control of Scientific and Engineering Software. All post processing was done using TECPLOT® 360™ Version 2009 (TECPLOT, Inc., 2009).

References

ANSYS, Inc. "ANSYS FLUENT Version 12.1, User's Guide." Canonsburg, Pennsylvania: ANSYS Inc. 2009.

Das, K. and D. Basu. "Compiling MFIX in Sun Solaris Platform and CFD Simulation of Magma Dynamics." Scientific Notebook No. 825E. San Antonio, Texas: CNWRA. pp. 103–115. 2011.

TECPLOT, Inc. "TECPLOT 360 Version 2009." Bellevue, Washington: TECPLOT, Inc. 2009.

1 INTRODUCTION

This report describes work supporting U.S. Nuclear Regulatory Commission activities on potential geologic disposal of commercial spent nuclear fuel and high-level radioactive waste. The report provides previously undocumented results for recent numerical simulations for cooling of magma as a lava flow. This report presents results of simulations carried out to evaluate the dynamics involved in cooling long individual sheet lobes of lava after they become stagnant. The simulations employ a geometry that consists of a hot lava body overlying a cool substrate of lava and other rock. The investigation also analyzes the effect of the convective heat transfer coefficient and the effect of temperature-dependent thermal conductivity and density on the temperature distribution. Computed results demonstrate that the core temperature decreases significantly after 2 years. As lava cools with time, the liquid core thickness decreases and the solidified crust thickness increases.

The essence of the numerical analysis is related to the cooling of hot bodies in the natural environment (e.g., on the surface, influenced by wind and rain, or under the surface, influenced by rock and groundwater). The current study and analysis can be applied to any cooling hot body where conduction dominates internal heat loss but radiation to and convection in the outside environment aids surface cooling. Convection is not predicted to occur inside the hot body being considered (lava, in this case), but some results suggest that convection may occur under some circumstances. This work aims to assess how lava flow cooling can be modeled, accounting for variability within the natural environment during the time taken to cool to the ambient temperature. Part of the purpose of this modeling is to compare results obtained by applying a fluid dynamics code with those of other numerical analyses using a quasi-two-dimensional approach; similar rates and cooling times for the cooling of basalt lava are obtained by this alternative modeling approach. Another objective of the current work is to investigate the effect of lava viscosity modeling on the cooling history, temperature profiles, and solidification of the lava. Simulations have been carried out using both constant and variable parameters, and the effects of these parameters on the predicted solution have been analyzed.

1.1 Background

Lava flow cooling has been an area of active research interest over the last few decades. Lavas develop cooled crusts while being emplaced; the upper crust is generally thicker than the lower in cooled lava units (Keszthelyi and Denlinger, 1996, Patrick, et al., 2004). Several researchers in the past (Shaw, et al., 1977; Peck, et al., 1977; Keszthelyi and Denlinger, 1996; Neri, 1998; Keszthelyi, et al., 2003) studied different aspects of lava cooling. Numerical simulations of lava cooling involve a number of assumptions for the different thermodynamic processes that dominate the cooling process as well as the material properties that define the lava characteristics. Shaw, et al. (1977) and Peck, et al. (1977) developed one of the earliest numerical models for lava flow cooling using a simplified approach whereby the ground and lava were modeled as a stack of elements and the top and bottom of the stack were maintained at a constant 0 °C [32 °F]. The model accurately characterized the internal temperature of the Alae lava lake, Hawaii.

Keszthelyi and Denlinger (1996) developed a numerical model for lava cooling that included surface cooling by both thermal radiation and atmospheric convection. The developed model realistically predicted the cooling rates of pahoehoe flows under different conditions. Keszthelyi and Denlinger (1996) found that while thermal radiation is the dominant initial heat loss mechanism, atmospheric convective cooling also plays an important role, even in the initial cooling stages. The numerical approach Neri (1998) developed allowed the investigation of the

main variables and parameters affecting the cooling process of a thermal-diffusion-dominated lava flow. This approach (Neri, 1998) also determined that surface features can strongly influence the global heat transfer between lava and atmosphere as well as the local cooling history of the flow. Keszthelyi, et al. (2003) used observational data to investigate the effect of wind speed on lava flow cooling. Comparison of the observed results to predictions from a wide range of convection formulas showed that (i) there is a general agreement between the predictions and observations and (ii) the effectiveness of free convection may have been underestimated in the past (Keszthelyi, et al., 2003). Several other past studies also addressed different aspects of lava cooling. These include Head and Wilson (1986), who looked at Venus flows; Ishihara, et al. (1990) and Dragoni (1989), who based their analysis on the assumption of radiation-dominated cooling; and Crisp and Baloga (1990), who characterized a'a lava surface heat losses. Young and Wadge (1990) developed a numerical program to model the path of flowing lava. Wooster, et al. (1997) carried out a detailed examination of the complete thermal budget of Etnean flows.

While the majority of the past work has focused on cooling lava elements by an analytical and seminumerical approach, the present work has focused on an analysis based on solving Navier-Stokes equations. In addition, none of the previous work on *in-situ* cooling of lava has explored the effect of lava viscosity on lava cooling. The present work has systematically explored the importance of variable parameters on the predicted temperature field. Simulations were carried out with variable viscosity, constant viscosity, variable thermal conductivity, and variable density.

The computational domain consists of a two-dimensional rectangular slab. A wide lava body of constant thickness is considered in the current simulations. This implies that the lava is sheetlike, and although the computation grid is limited, there are no edge effects. The current work, although carried out for simulating lava flow cooling, can be applied to any situation involving cooling of a hot body where conduction dominates internal heat loss, but radiation to and convection in the outside environment aids surface cooling. The influence of the substrate underlying the hot lava body (consisting of carbonate rock overlain by a layer of previously solidified cold lava) on the cooling pattern is also analyzed.

This analysis also explores whether the influence of rain and the convective heat transfer coefficient makes any significant long lasting impact on the temperature pattern. The influence of wind is simulated through an ambient temperature boundary condition at the top. The air is assumed to be static with an ambient temperature and acts as a heat sink. The effect of heated air being transported and subsequently replaced by colder air is not considered in these simulations. The computational models developed at the Center for Nuclear Waste Regulatory Analyses (CNWRA®) are based on some prior thermal analysis of lava cooling (Patrick, et al., 2004) carried out for flows produced during the 1997 Okmok, Alaska, eruption.

1.2 Purpose and Scope

This summary report documents the important technical aspects and results of computational analyses designed to investigate the cooling of hot lava on the Earth's surface under different environmental conditions. The models are not designed to simultaneously simulate the flow of lava and its cooling, but rather the conditions when hot stagnant lava is cooling in contact with the ground (e.g., previously solidified lava flow units or another rock type). CNWRA staff conducted these numerical simulations to better understand and develop critical insights into the long-term (~3 years) thermal behavior of hot bodies in contact with the cold (ambient) ground and air in natural conditions. Results presented in this report support prior observations and

measurements (Patrick, et al., 2004; Hon, et al., 1994) of lava cooling at actual volcano sites. To analyze the thermal field and evaluation of cooling, the work is restricted to two-dimensional numerical simulations under conditions of transient cooling analysis. No non-Newtonian viscosities, such as Bingham-Plastic, are assumed for the stagnant, cooling lava. Instead, values and correlations obtained from prior investigations (Patrick, et al., 2004; Keszthelyi and Denlinger, 1996) involving viscosity and thermal conductivity of basaltic lavas are used in the current analysis. Assuming a constant viscosity with a variable thermal conductivity and variable density results in some nonrealistic plumelike structures appearing in some simulations, but the overall time scale of cooling is not much affected by this. On the other hand, simulations with all variable properties (viscosity, density and thermal conductivity, as occurs in the natural system) show development of Rayleigh-Taylor instability from the lower part of the developing upper crust. Based on the two-dimensional simulations, salient features can be captured and parametric analysis can be carried out at a considerably reduced computational burden using the ANSYS® FLUENT™ (ANSYS, Inc., 2009) fluid dynamics software package.

2 METHODOLOGY

2.1 Model Geometry

As noted earlier, the configuration modeled in this study is restricted to two dimensions. Figure 2-1 shows a 20- to 80-m [66- to 262-ft] computational domain that is chosen for the present computations. The configuration consists of 50 m [164 ft] of thick, hot lava at the top. Below the hot lava, there is one substrate layer of cooled, solidified lava 15 m [49 ft] in thickness. Below this solidified lava is cold ground 15 m [49 ft] in thickness. The thicknesses are chosen based on the values Patrick, et al. (2004) used in similar prior calculations. The computational domain consists of a two-dimensional rectangular slab. A wide lava body of constant thickness has been considered in the current simulations. The edge effect is avoided by applying the periodic boundary condition.

The geometry of the configuration and the computational domain is provided in Table 2-1.

2.2 Computational Grid and Boundary Conditions

The two-dimensional uniform computational grid used in these simulations consists of 10,000 rectangular cells (Figure 2-2). Table 2-2 details the grid dimensions for each geometric construct. No clustering of the grid is employed near the wall regions. However, the computational grid in the vertical direction is clustered near the top boundary of the hot lava and at the intersection of the hot lava with the substrate (the middle lava layer). This is done to efficiently capture the thermal gradients in those regions.

A periodic boundary condition is used in the horizontal x direction. The periodic boundary condition is used to implement the repetitiveness of the solution in the lateral direction. This boundary condition enables more realistic simulation of an infinite length of a sheetlike lava body. In addition, no heat transfer is considered in the horizontal direction. For the top surface, a mixed convection–radiation boundary condition is used. Prior investigations (Keszthelyi and Denlinger, 1996; Neri, 1998; Keszthelyi, et al., 2003) demonstrated that heat transfer from the lava surface is dominated by both convection and radiation; hence we use a mixed boundary condition at the top. The heat transfer from the top is assumed to be taking place through the combination of convection and radiation, and the convective heat transfer coefficient, as well as the emissivity, is specified. Heat transfer between the hot lava and the cold lava substrate, and subsequently to the rock substrate layer, is through conductive heat transfer. The initial temperature is 1,500 °K [2,240 °F] for the hot lava, while the substrate and the ground are considered to be at a normal ambient temperature of 293 °K [68 °F].

The present simulations do not specifically take into account the wind velocity in the air above the hot lava. The effect of replacing warmed air above the hot lava body with colder air is implemented through maintaining the ambient temperature at 305 °K [89 °F]. The heat transfer between the top surface of the hot lava and the atmosphere is assumed to be controlled by the convective heat transfer and the radiation parameters. Prior investigations on external cooling of lava flows (Neri, 1998; Keszthelyi, et al., 2003) determined that in the initial stages of cooling there exists a substantial temperature difference between hot lava and the air above it. However, subsequent radiative heat loss quickly reduces the temperature of the lava top surface to values approaching those of the ambient temperature.

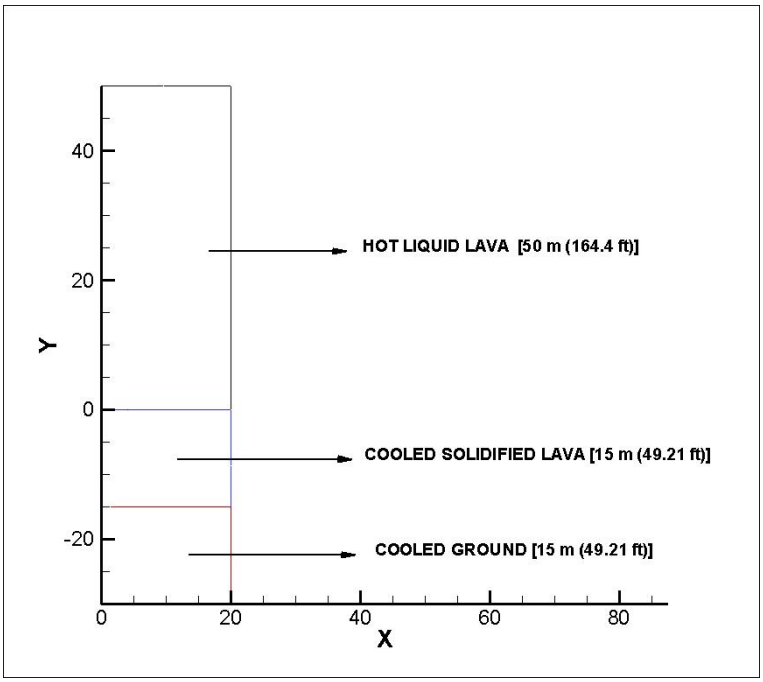

Figure 2-1. Schematic of the Modeled Lava–Ground Configuration; Length Is in Meters: Note that the Hot Lava Base Is at 0 m and the Depth Into Substrate Is Indicated as Negative Values

Table 2-1. Model Construct Values	
Construct	**Thickness Value**
Hot lava crust (at the top)	50 m [164 ft]
Cold lava (middle layer)	15 m [49 ft]
Cold ground/rock (bottom layer)	15 m [49 ft]

This boundary condition is assumed for all the cases where the effect of rainfall is not considered. The effect of rainfall is accommodated by increasing the heat loss per time, as explained next.

For the simulation cases where the effect of rainfall is considered, the top surface boundary condition is changed to accommodate this condition. Patrick, et al. (2004) and Shaw, et al. (1977) detailed the effect of rainfall on the lava cooling. According to Patrick, et al. (2004), rain that contacts the hot upper surface will vaporize and extract heat from the flow at the top surface. The present set of computations with rainfall models the effect of rain through this latent heat of vaporization concept. This model with rain simulation is based on the prior observations by Shaw, et al. (1977). In their model, all rain contacting the top surface is assumed to vaporize completely. This enables the calculation of the latent heat of water vaporization in addition to a measurement of the heat required to raise the temperature of water from the ambient value to 100 °C [212 °F]. This total heat amount is subtracted from the top surface of the hot lava body. In the ANSYS-FLUENT model, the top surface is assigned as a heat sink, from where heat is extracted, in the simulation cases with rainfall.

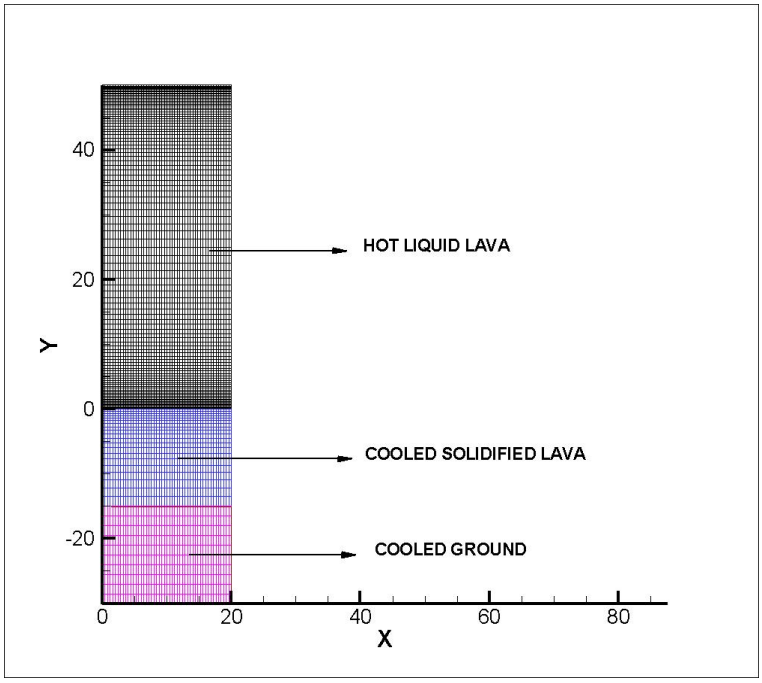

Figure 2-2. Schematic of the Computational Grid Used in the Simulations: Different Zones Are Shown in Different Colors and Length Is in Meters

Table 2-2. Details of the Computational Grid	
Construct	**Grid Dimension ($N_x \times N_y$)***
Hot lava thickness (at the top)	50 × 120
Cooled lava crust thickness (middle layer)	50 × 40
Cooled ground thickness (bottom layer)	50 × 40
*N_x = Number of cells in the x direction and N_y = number of cells in the y direction	

The radiative heat transfer is calculated using the Stefan-Boltzmann equation [Eq. (2-1)]

$$Q_r = \sigma\varepsilon[T_h^4 - T_c^4] \qquad (2\text{-}1)$$

where σ is the Stefan-Boltzmann Constant given as 5.67×10^{-8} W m^{-2} K^{-4} [0.1714×10^{-8} BTU h^{-1} ft^{-2} R^{-4}]; ε is the emissivity for radiation and is taken as 0.95 in the present computations; T_h is the hot lava surface temperature; and T_c is the ambient temperature. The convective heat transfer is calculated through Newton's law of cooling. The value for the convective heat transfer coefficient is taken as 50 W/m^2 K [8.83 BTU h^{-1} ft^{-2} °F^{-1}].

2.3 Material Properties

Simulations are carried out for lava with constant properties as well as variable properties. The values of properties for the lava are based on data available in the open literature (Keszthelyi and Denlinger, 1996; Neri, 1998; Keszthelyi, et al., 2003; Patrick, et al., 2004). For simulations with constant properties of lava, the values of the different properties are listed in Table 2-3. These primarily are based on the values Patrick, et al. (2004) provided.

For simulations with variable properties of lava, the following formulations are used for thermal conductivity and density. These formulations are obtained from the work by Keszthalyi (1994) and were based on the laboratory data for basalt from Touloukian, et al. (1989). The formulations for thermal conductivity and density are given in Eqs. (2-2) and (2-3)

$$K(T) = 0.427 + (772/T) - (8.72 \times 10^4/T^2) \quad (2\text{-}2)$$

$$\rho(T) = \rho_0/[1 + \beta(T\text{-}1450)] \quad (2\text{-}3)$$

Here ρ_0 is the initial density and β is the volumetric coefficient of thermal expansion and is taken as $1.5 \times 10^{-5}\ K^{-1}$.

The variable viscosity formula used in the simulations is based on the analysis by Costa and Macedenio (2005, 2003) The formulation for the viscosity is given by Eq. (2-4)

$$\mu\ (T) = \mu_r \exp\ [-b^*(T\text{-}T_r)] \quad (2\text{-}4)$$

In this formula, b is an appropriate rheological parameter and μ_r is the viscosity value at the reference temperature T_r. The present simulations use the following values for the parameters. The model values are obtained from Costa and Macedenio (2005, 2003)

$$\mu_r = 1{,}000 \text{ Pa-s } (21 \text{ lbf-s/ft}^{2)} \quad (2\text{-}5)$$
$$b = 0.02\ K^{-1}$$
$$T_r = 1{,}350\ ^\circ K\ (1970.33\ ^\circ F)$$

2.4 Numerical Methods

The commercial software ANSYS FLUENT Version 12.1 (ANSYS, Inc., 2009) is used for the simulations. FLUENT uses a control-volume-based technique to convert a general scalar transport equation to an algebraic equation that is solved numerically. It has a pressure-based solver and a density-based solver. While the pressure-based solver is normally used for incompressible flows, the density-based solver is recommended for compressible high Mach number flows. A variety of spatial and temporal discretization schemes, as well as turbulence models, is also available in ANSYS-FLUENT.

For these simulations, the solutions to the full two-dimensional Navier Stokes equations are obtained using an unsteady, implicit approach. The Semi-Implicit Pressure Linked Equations Consistent (SIMPLEC) algorithm (Van Doormal and Raithby, 1984) is used to treat pressure–velocity coupling for stability. The third-order Monotone Upstream-Centered Schemes for Conservation Laws (MUSCL) (Van Leer, 1979) scheme is used to derive the face values of different variables for the spatial discretization; these variables are used to compute the convective fluxes. The upwind difference scheme is used for its enhanced numerical stability. The pressure-based solver is used in conjunction with the Green-Gauss cell-based gradient option. An implicit time-marching scheme is used for faster convergence. Temporal discretization is achieved through a second-order implicit method (second-order backward Euler scheme) (Gresho, et al., 1980). The solutions assumed a Newtonian viscosity for the lava. Non-Newtonian viscosity is not included in the models and the simulations. The solutions are initiated in the unsteady mode. The timestep used for the unsteady simulations varied between 0.01 and 0.1 days. The computations are conducted on a Sun Fire X4100 cluster configured with 10 dual-core AMD Opteron 200 series processors with 16 GB RAM per processor.

Table 2-3. Materials and Properties Used in the Simulations								
	Density		Specific Heat		Thermal Conductivity		Viscosity	
	Kg/m^3	lbm/ft^3	J/kg-K	BTU/lb-°F	W/m-K	Btu/(ft h °F)	Pa-s	$lbf\text{-}s/ft^2$
Lava (Hot)	2,600	162.31	1,100	0.262	1.2	0.69	100	2.1
Lava (Solidified Cooled Substrate)	3,000	187.28	840	0.20	1.2	0.69	—	—
Ground	2,800	174.78	856	0.20	2.25	1.3	—	—
	J/kg	BTU/lb	°K	°F	°K	°F	°K	°F
Lava (Hot)	350,000	150.47	1,273	1831.73	1,473	2191.73	1,500	2,240
Lava (Solidified Cooled Substrate)	—	—	—	—	—	—	300	80
Ground	—	—	—	—	—	—	300	80

3 RESULTS AND DISCUSSIONS

To gain insights about the effect of different parameters on the lava cooling history, the degree of solidification, and associated thermal fields, current simulations focused primarily on three scenarios: (i) lava cooling with constant viscosity, constant thermal conductivity, and constant density; (ii) lava cooling with constant viscosity, variable thermal conductivity, and variable density; and (iii) lava cooling with variable viscosity, variable thermal conductivity, and variable density. In addition, simulations are carried out for lava cooling under the influence of rainfall.

After the baseline simulations with constant lava properties, which make the solution computationally simpler, simulations are carried out with variable thermal conductivity and variable density but with constant viscosity. That simulation produces unphysical results that can be attributed to keeping the viscosity constant while varying the two other properties. Excluding a temperature-dependent viscosity probably results in some unrealistic convection patterns in the hot lava core region. Hence, additional simulations are carried out with a temperature-dependent viscosity along with temperature-dependent density and thermal conductivity. The effect of lava viscosity on the predicted temperature field is analyzed. For each of the cases with constant and variable properties, we also consider subcases that include the effect of rain. These cases are chosen as end members to carry out this preliminary analysis. The degree of cooling through the change in temperature and the degree of solidification through the change in liquid fraction are investigated. The value of the convective heat transfer coefficient is taken as 50 W/m^2K [8.8 BTU h^{-1} ft^{-2} $°F^{-1}$] for the majority of these simulations. However, in the end, a parametric analysis is also carried out to evaluate the effect of convective heat transfer on the temperature and associated cooling pattern. No parametric analysis is carried out with variable properties.

3.1 Baseline Simulation Results

Baseline simulations refer to the computations with constant viscosity, constant thermal conductivity, and constant density. Figures 3-1 through 3-6 show the results obtained from these simulations. Figure 3-1 shows the contours of the static temperature at different times over a 30-month period. Results presented in Figure 3-1 are obtained with simulated rainfall. Note that (i) the temperature at the top decreases with increase in time and (ii) the dimension of the region at the top with a lower temperature (i.e., the developing upper crust to the lava body) increases as the numerical solution progresses in time. The temperature at the top of the cooling lava crust approaches that of the ambient temperature after 18 months. A thinner lower lava crust also develops above the contact with the substrate. In addition, note that the cold substrate layer below the hot core region has an increase in temperature, which is significant to several meters' [ft] depth. After 30 months, there is a temperature difference of almost 200 °K [100 °F] between the lowermost substrate temperature and the layer in the core of the lava 20 m [66 ft] above it. Figure 3-1 clearly shows that the upper layer cools down with time through heat transfer at the top, while the bottommost ground layer and the cooled lava substrate get heated up in contact with the hot lava. Significant solidification and gradual thickening of the bottom part of the hot lava core can be observed in contact with the cold lava substrate layer.

The degree of solidification is shown in Figure 3-2 through the contours of the liquid fraction. Note the gradual progression of the solidification front with time at both the top and bottom surface, and the faster development of the upper crust on the hot lava. As the top layer starts to cool down, gradual solidification begins at the top layer, which slowly progresses downward with

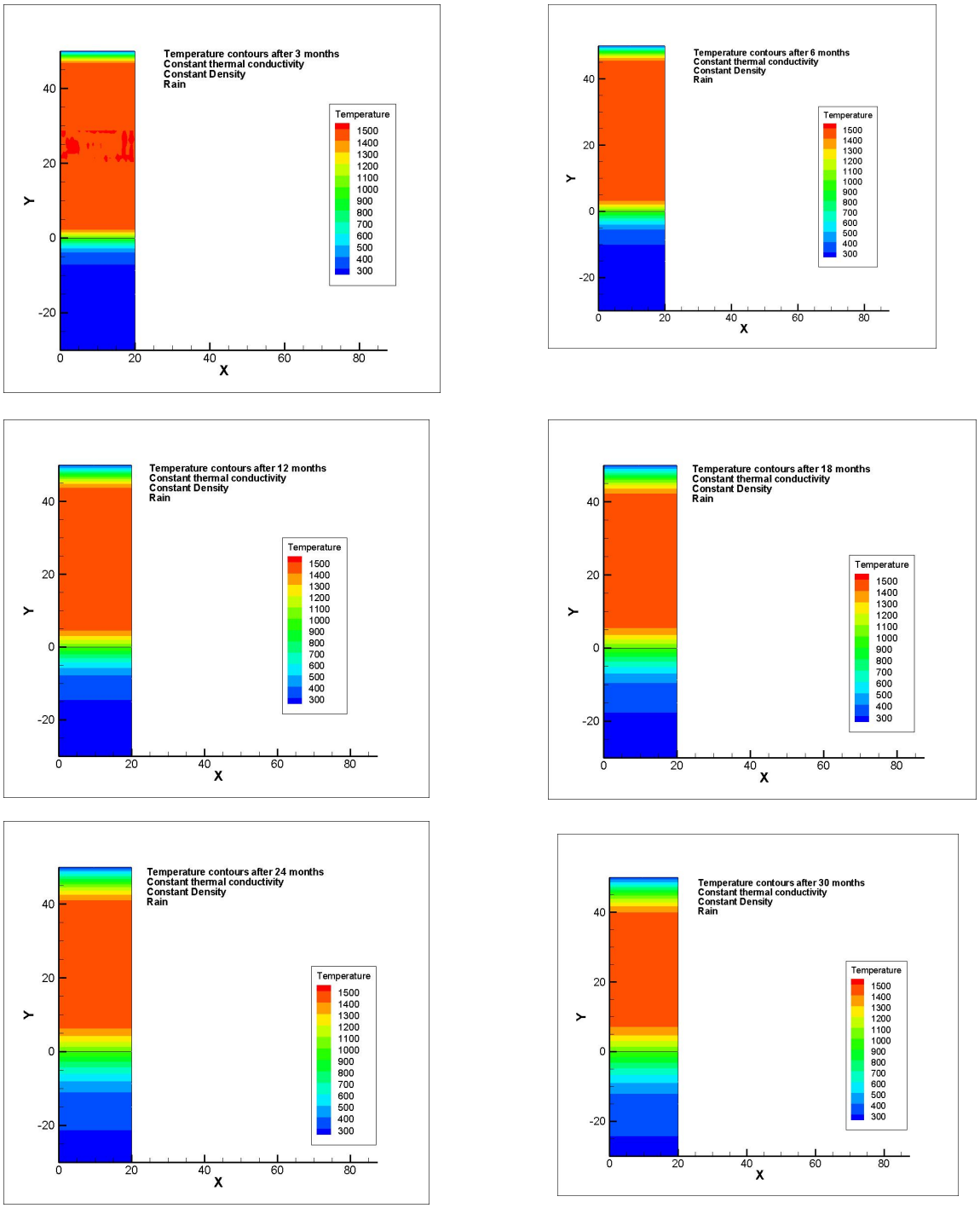

Figure 3-1. Contours of Static Temperature for Lava Cooling at Various Times: Simulations With Constant Thermal Conductivity, Constant Density, and Rain

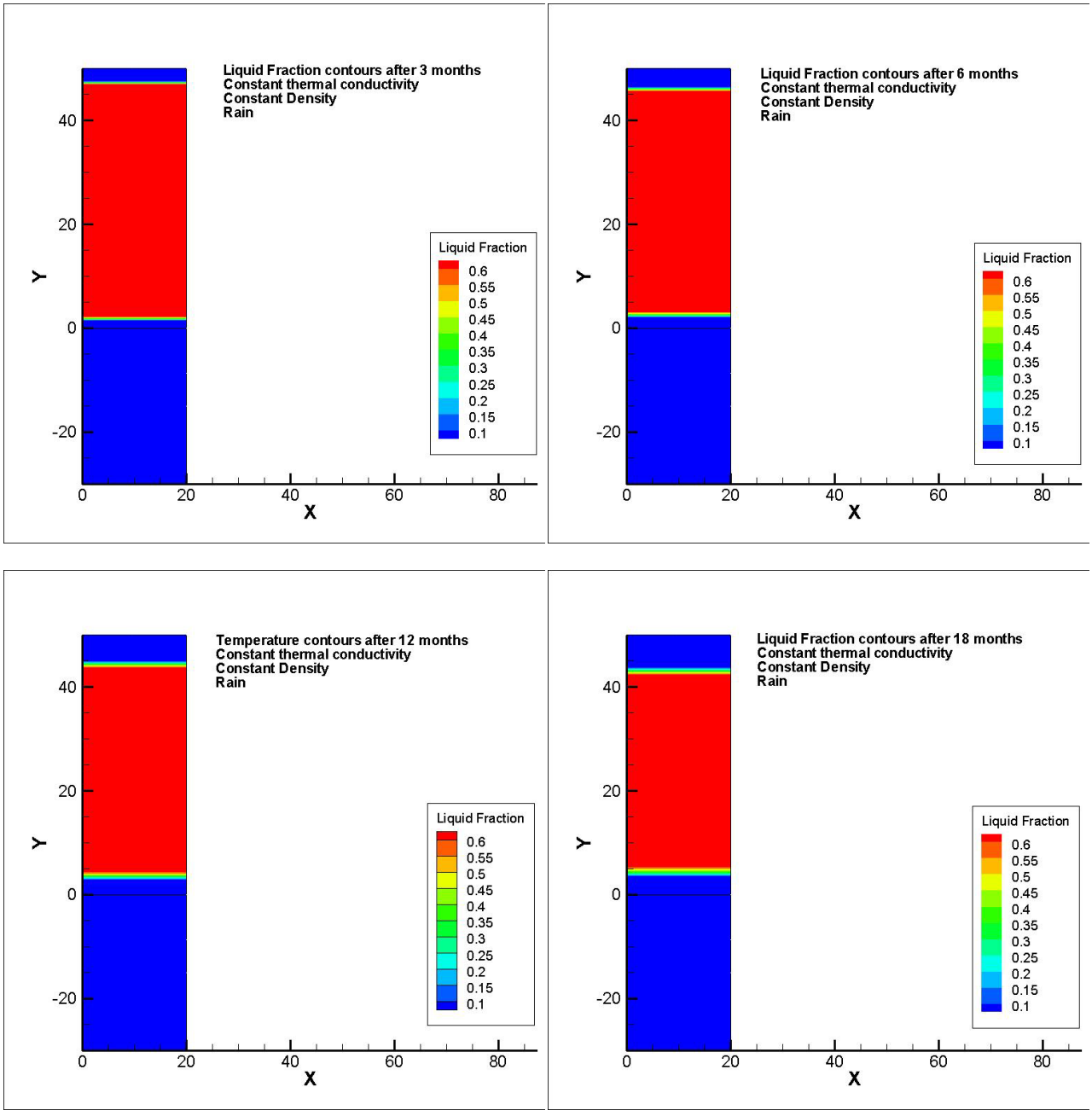

Figure 3-2. Liquid Fraction Contours Showing the Degree of Solidification for Lava Cooling at Various Times: Simulations With Constant Thermal Conductivity, Constant Density, and Rain

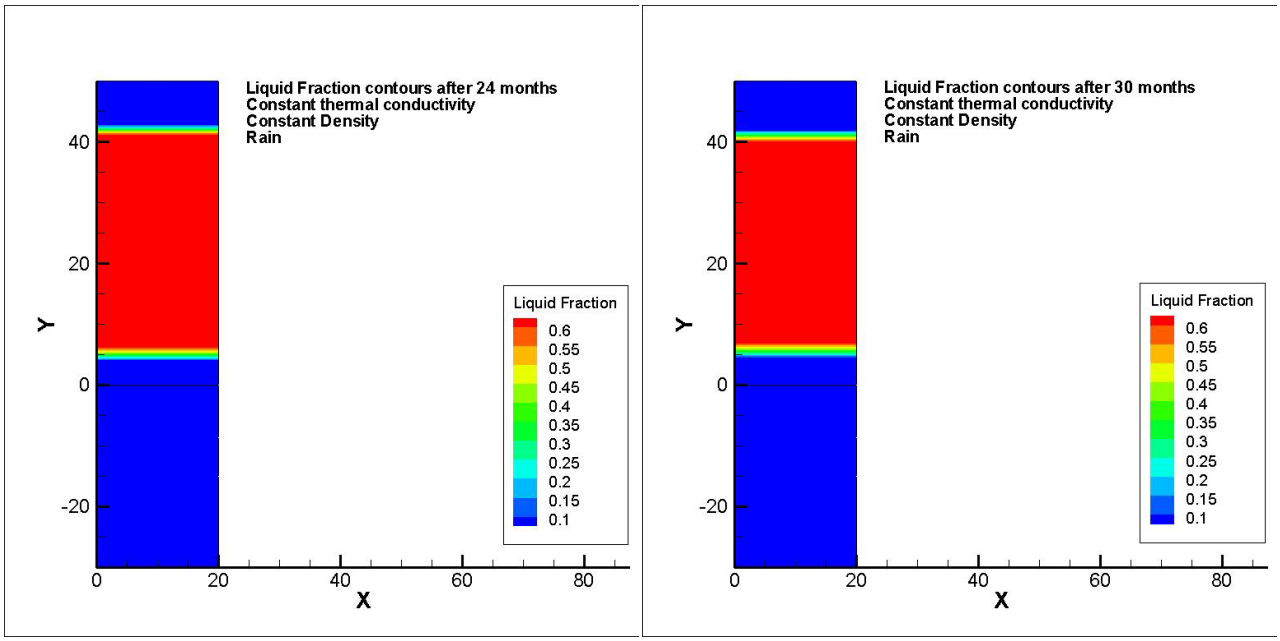

Figure 3-2 (continued). Liquid Fraction Contours Showing the Degree of Solidification for Lava Cooling at Various Times: Simulations With Constant Thermal Conductivity, Constant Density, and Rain

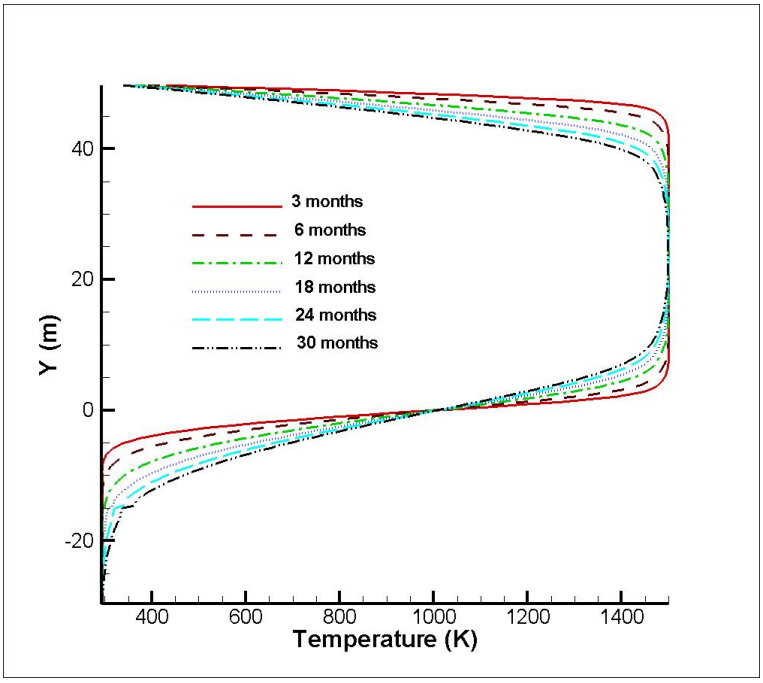

Figure 3-3(a). Variation of Internal Temperature Gradient for Lava Cooling: Simulations With Constant Thermal Conductivity, Constant Density, and Rain

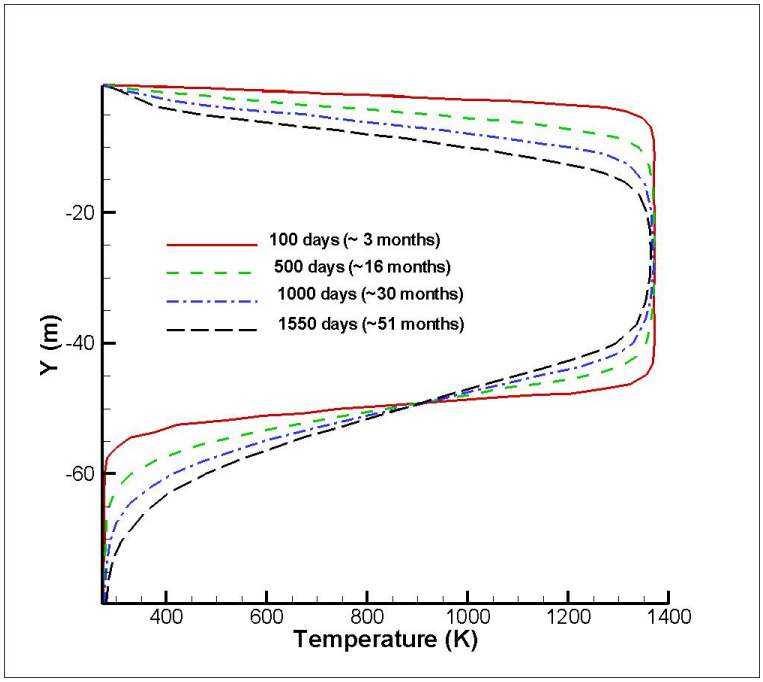

Figure 3-3(b). Variation of Internal Temperature Gradient for Lava Cooling: MATLAB Computation of Patrick, et al. (2004)

time. Simultaneously, the hot core lava in contact with the substrate begins to solidify. After 30 months, the thickness of the solidified lava zone at the top is almost 10 m [33 ft], while the solidification zone at the intersection of the hot core and the cold substrate measures almost 5 m [16 ft]. Figures 3-1 and 3-2 show that any hot body in contact with a cooler body begins to lose heat through conduction at the point of contact and significant heat transfer can take place, which may lead to a change of phase through solidification.

Figure 3-3 shows the variation of the internal temperature gradient with lava cooling as a function of time, which provides insight about the flow interior and the insulating properties of lava. As the figure shows, the 30-m [98-ft]-thick portion of the lava core maintains a constant temperature of nearly 1,480 °K [2,204 °F] even after 30 months. However, the top and the bottom layer of the lava core undergo significant changes in temperature and crust formation. As can be observed in Figure 3-3(a), the top and the bottom layers of the hot lava core undergo changes in temperature almost at the same rate with time. Figure 3-3(b) shows similar data obtained from the MATLAB simulations of Patrick, et al. (2004), depicting the modeled temperature gradient over a period of 1,550 days (~51 months). The nature of the temperature distribution obtained from the current simulations matches qualitatively well with the values Patrick, et al. (2004) obtained. This is because in the current simulations, which are carried out with a periodic boundary condition in the lateral (x) direction, no thermal variation occurs in the x direction. Hence, this problem essentially reduces from a two-dimensional problem to a one-dimensional problem (i.e., one without variations in the horizontal x direction). This new simulated result compares well with that of Patrick, et al. (2004), which was also essentially a one-dimensional solution.

Figure 3-4 shows contours of the static temperature at different times over a 30-month period for simulations with no rainfall. Comparing Figure 3-4 with Figure 3-1 shows that the inclusion

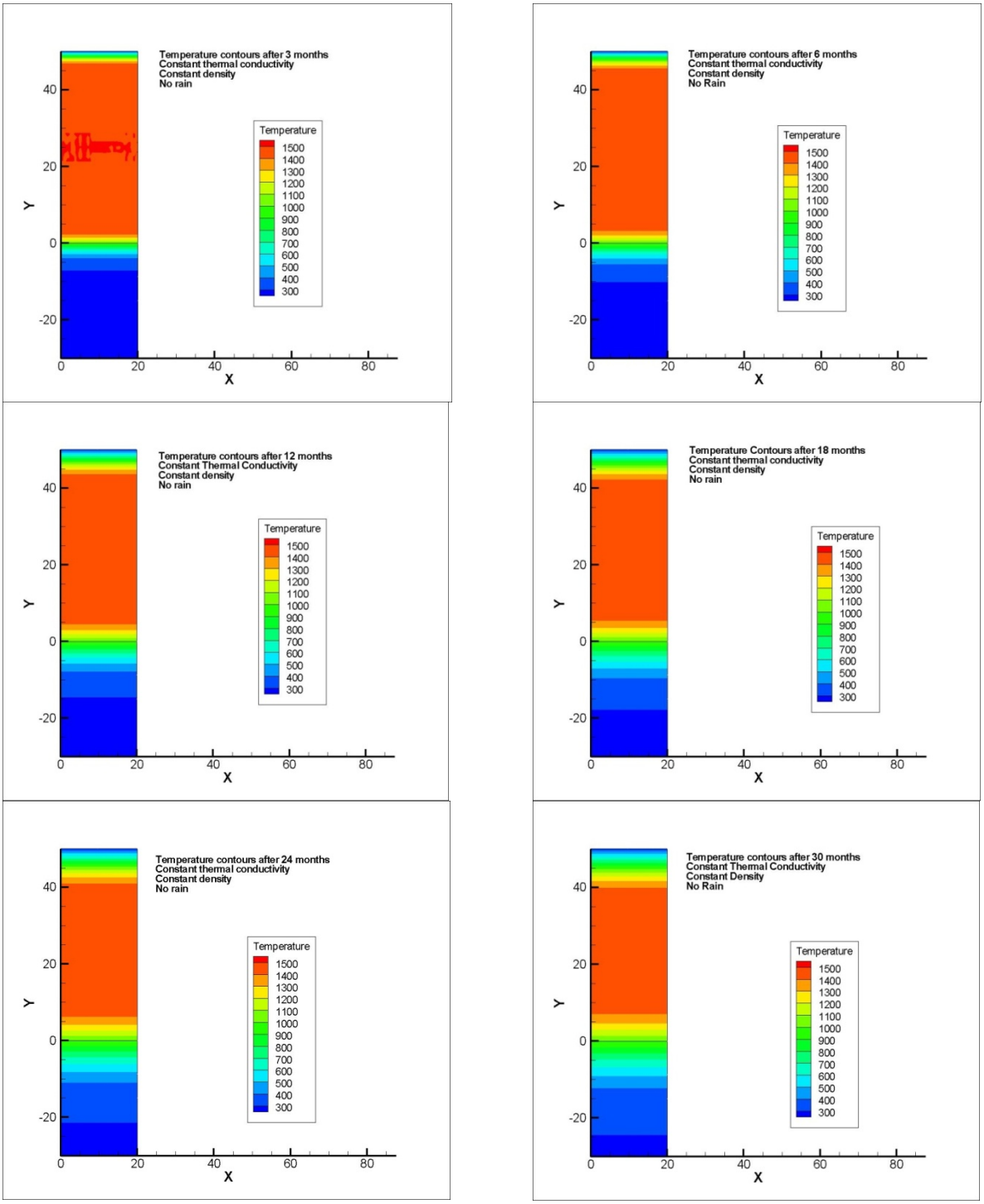

Figure 3-4. Contours of Static Temperature for Lava Cooling at Various Times: Simulations With Constant Thermal Conductivity, Constant Density, and No Rain

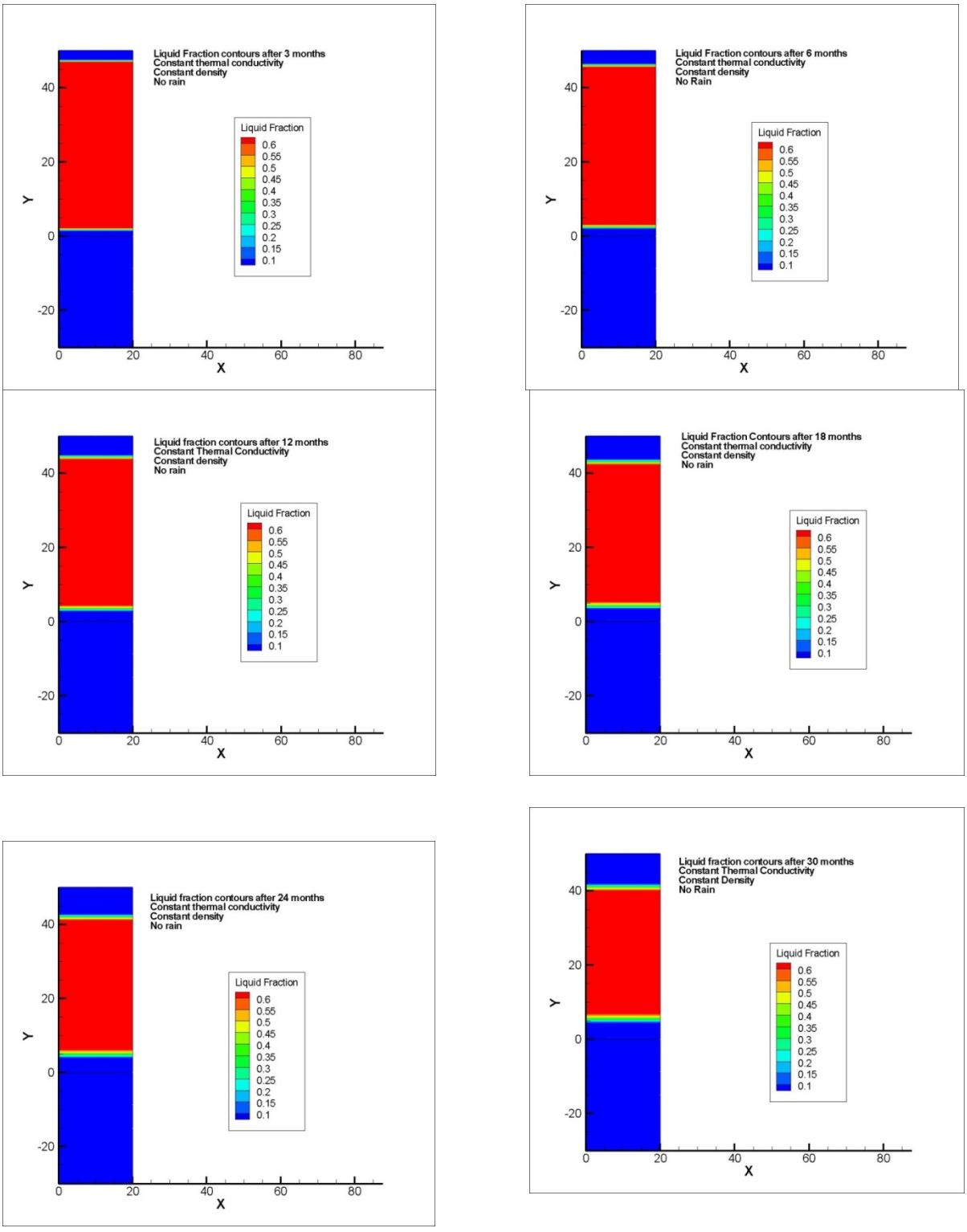

Figure 3-5. Contours of Liquid Fraction for Lava Cooling at Various Times: Simulations With Constant Thermal Conductivity, Constant Density, and No Rain

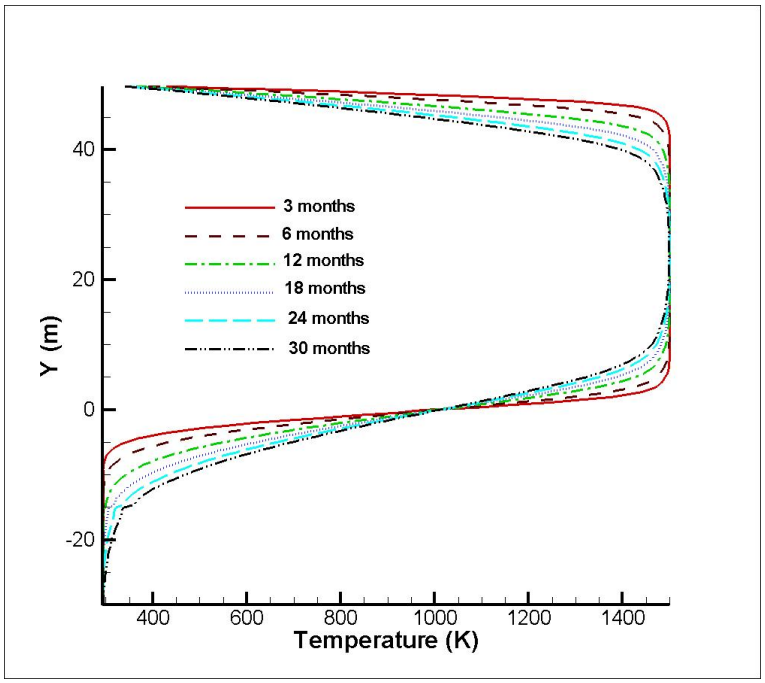

Figure 3-6(a). Variation of Internal Temperature Gradient for Lava Cooling: Simulations With Constant Thermal Conductivity, Constant Density, and No Rain

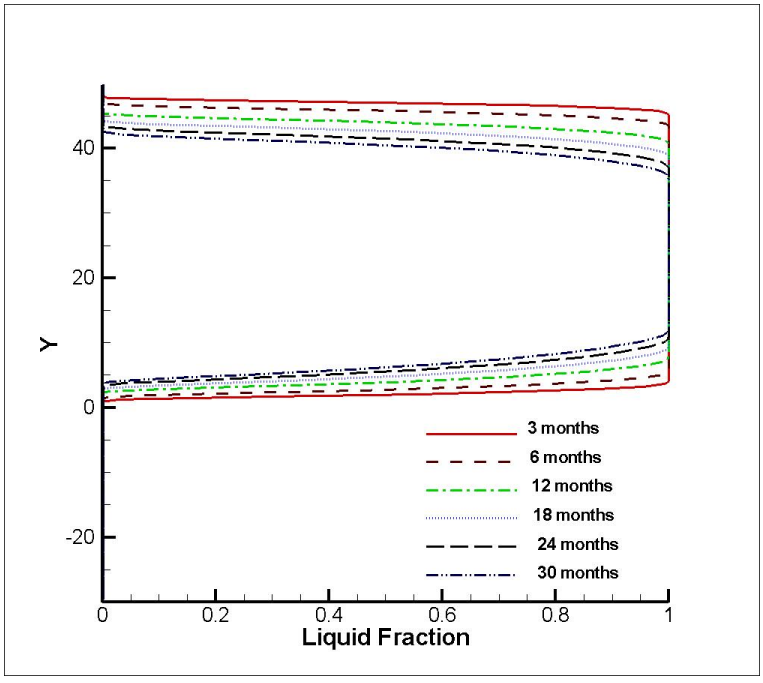

Figure 3-6(b). Variation of Liquid Fraction and Degree of Solidification for Lava Cooling: Simulations With Constant Thermal Conductivity, Constant Density, and No Rain

of rainfall has no significant effect on the static temperature distribution in cases with constant thermal conductivity and constant density. The temperature distribution as observed in Figure 3-4 is similar to that shown in Figure 3-1 for the simulations without rainfall. Similarly, Figure 3-5 shows that the degree of solidification for the simulations that take rainfall into account follows the same pattern exhibited by the simulations that do not take the rainfall into account.

The degree of cooling and the degree of solidification are shown in Figure 3-6(a) and 3-6(b), respectively, for the simulations that do not consider rainfall. Comparing Figure 3-6(a) with Figure 3-3(a) shows nearly identical temperature profiles; therefore, for simulations with constant thermal conductivity and constant density, rainfall has negligible influence on the temperature profile. The degree of solidification as shown in Figure 3-6(b) reveals that the solidified crustal layer at the top of the lava has a higher thickness compared to the solidified layer at the bottom. This is because at the top, heat transfer takes place through a combination of convection and radiation, whereas in the bottom regions, the only mode of heat transfer at the interface between hot lava and cooled crust is through conduction . Note that the 4–5 m [13-16 ft] of upper crust development with 4–6 months of cooling is in the same range as Hon, et al. (1994) observed for Kilauea lava lobes and shown in an empirical model.

3.2 Simulation Results With Variable Thermal Conductivity, Variable Density, and Constant Viscosity

Figures 3-7 through 3-12 show the results obtained from computations with variable thermal conductivity, variable density, and constant viscosity. As explained earlier, the variable thermal conductivity and variable density are chosen to reflect reality because these properties change as the lava cools. However, the viscosity is assumed constant throughout the simulations. Figures 3-7 through 3-9 illustrate the temperature and liquid fraction for simulations without rain, while Figures 3-10 through 3-12 illustrate the temperature and liquid fraction for simulations with rain. Figure 3-7 shows the contours of temperature at different time constants over a period of 30 months. A significant difference can be observed from the results obtained with constant thermal conductivity and constant density. The thermal field shows significant fluctuation and a plume-type structure developing over time. Note a vertical inhomogeneity in Figure 3-7. This can be attributed to the variable density of the lava generating vertical inhomogeneity through a convection pattern. As the simulations involve a constant, unchanging viscosity, no visco-elastic behavior is observed. The plume pattern can be attributed to the density changing with temperature while the viscosity remained constant. After 30 months, the temperature of the hot lava core decreases to 1,000 °K [1,340 °F] from an initial temperature of 1,500 °K [2,240 °F]. A comparison with Figure 3-1 shows that the simulations with variable thermal conductivity and variable density produce a significantly lower temperature for the hot lava zone compared to the simulations with constant thermal conductivity and density. This may be due to variable density that produces some type of convection pattern in the hot lava zone. As a result, significantly more heat transfer takes place compared to the constant thermal conductivity and constant density case, and consequently the temperature is reduced. Even though viscosity changes have been ignored, a crust develops more quickly compared to the case with constant properties.

Figure 3-8 shows the corresponding contours for the liquid fraction at various times for simulations with variable thermal conductivity and variable density. The figures at various times illustrate the rapid progress of the solidification front. After 30 months, almost the entire hot lava core has solidified. Figure 3-9 shows the variation of the internal temperature gradient and

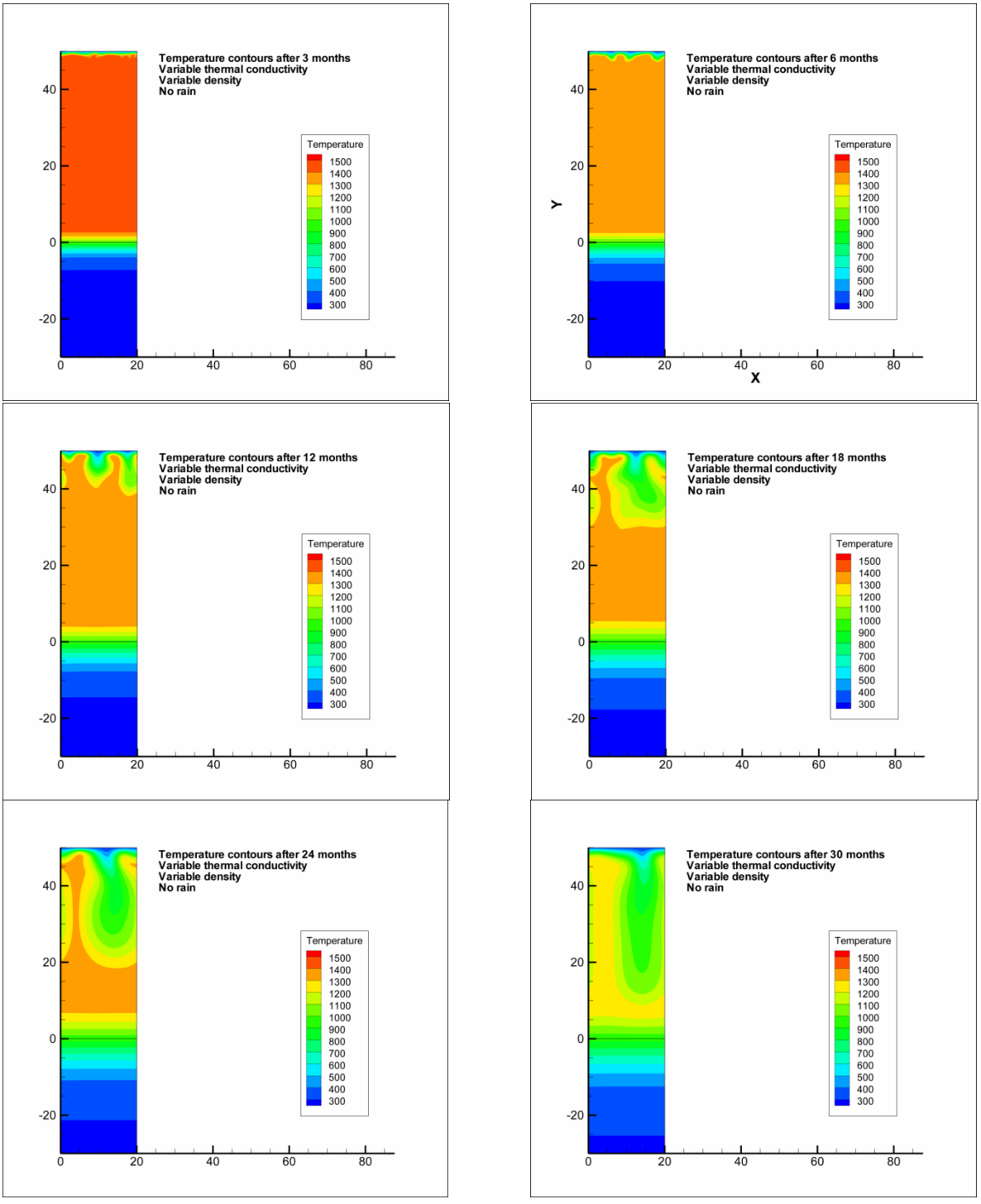

Figure 3-7. Contours of Static Temperature for Lava Cooling at Various Times: Simulations With Variable Thermal Conductivity, Variable Density, and No Rain

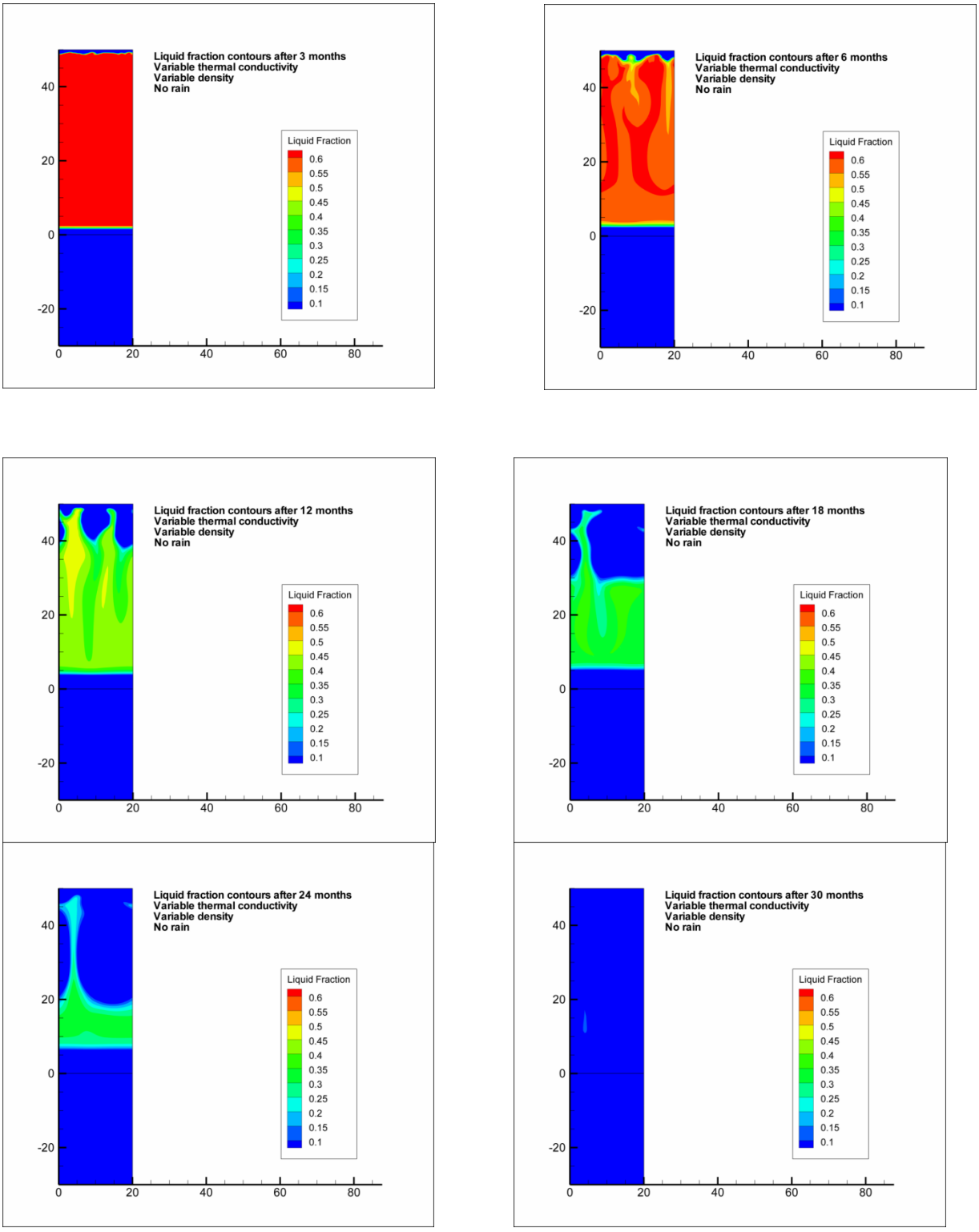

Figure 3-8. Liquid Fraction Contours Showing the Degree of Solidification for Lava Cooling at Various Times: Simulations With Variable Thermal Conductivity, Variable Density, and No Rain

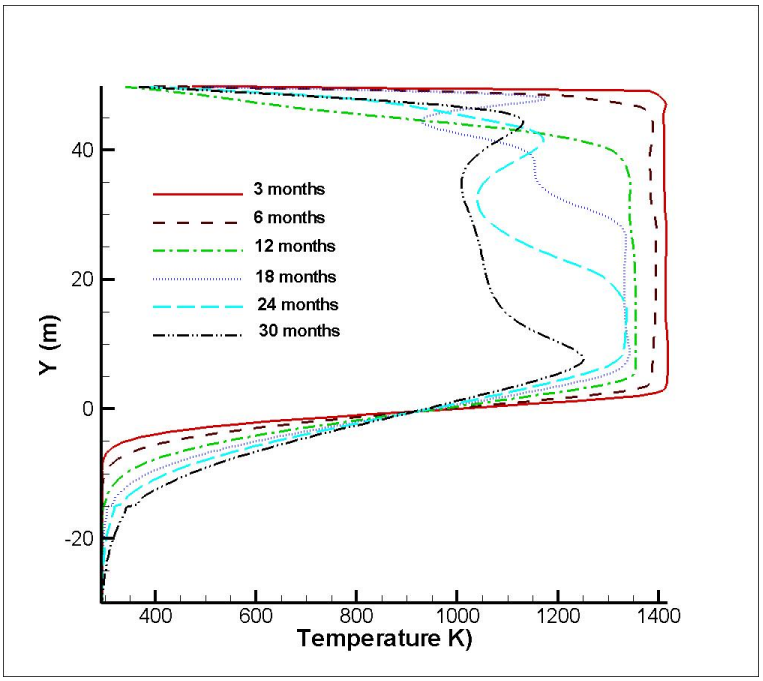

Figure 3-9(a). Variation of Internal Temperature Gradient for Lava Cooling: Simulations With Variable Thermal Conductivity, Variable Density, and No Rain

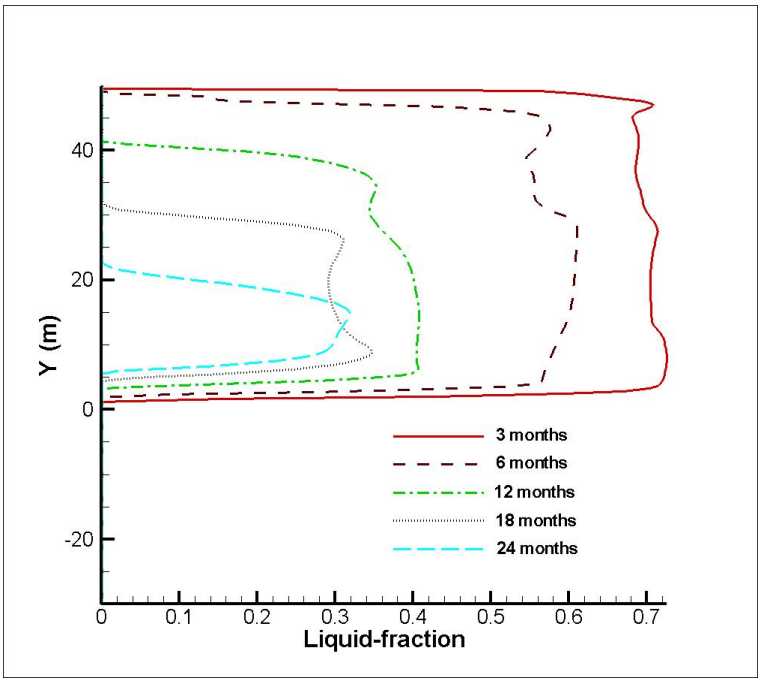

Figure 3-9(b). Variation of Liquid Fraction and Degree of Solidification for Lava Cooling: Simulations With Variable Thermal Conductivity, Variable Density, and No Rain

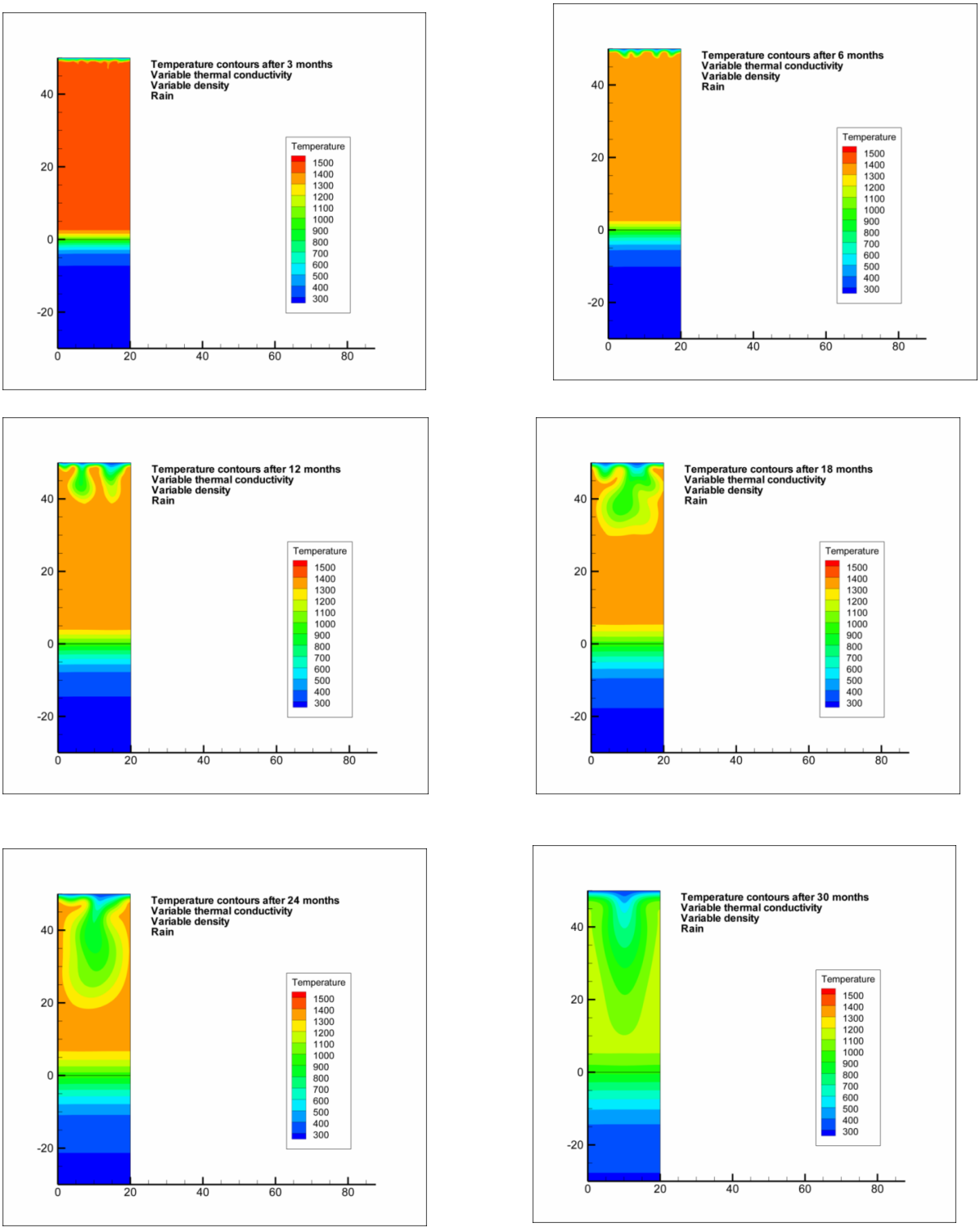

Figure 3-10. Contours of Static Temperature Showing the Degree of Lava Cooling at Various Times: Simulations With Variable Thermal Conductivity, Variable Density, and Rain

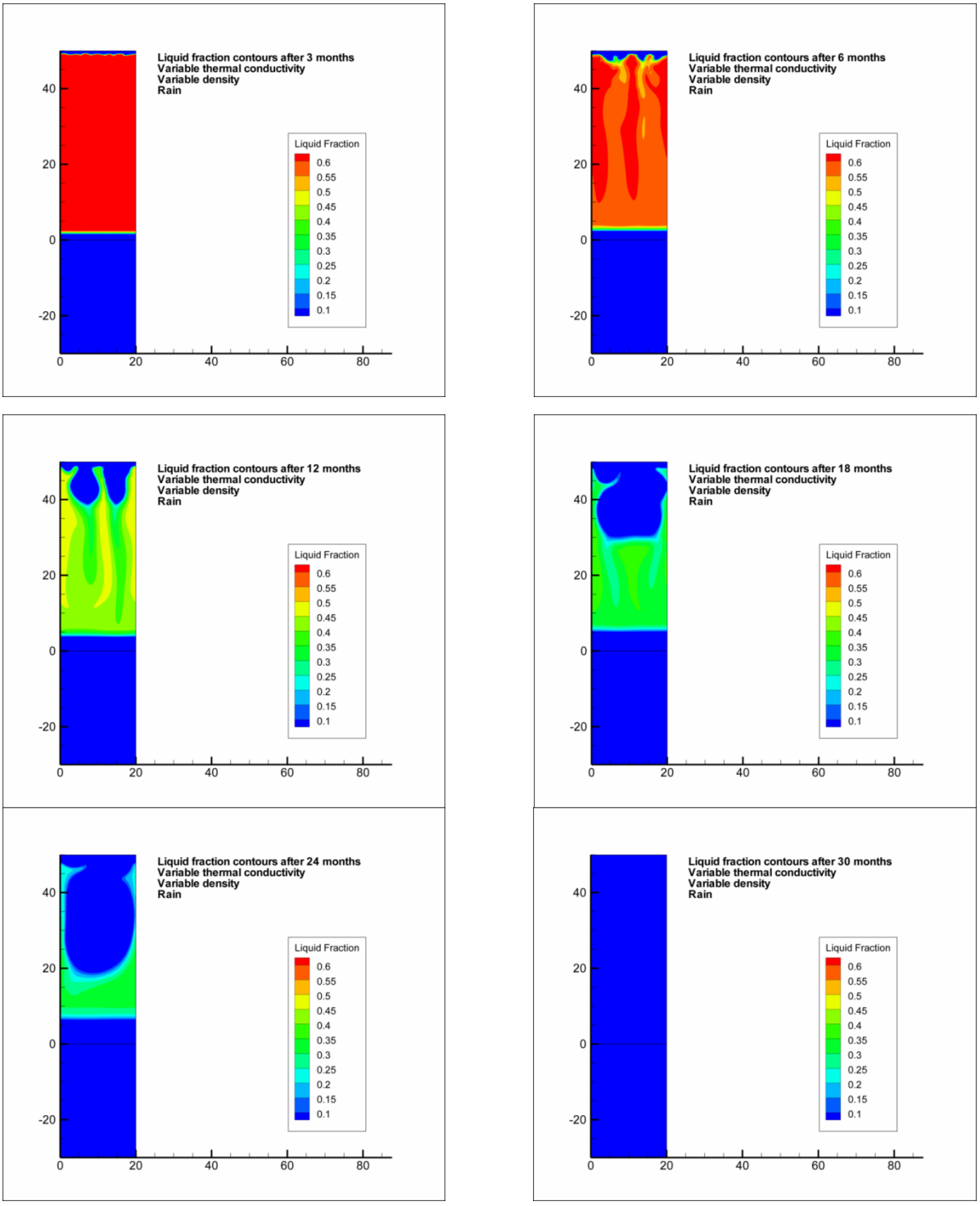

Figure 3-11. Contours of Liquid Fraction Showing the Degree of Lava Solidification at Various Times: Simulations With Variable Thermal Conductivity, Variable Density, and Rain

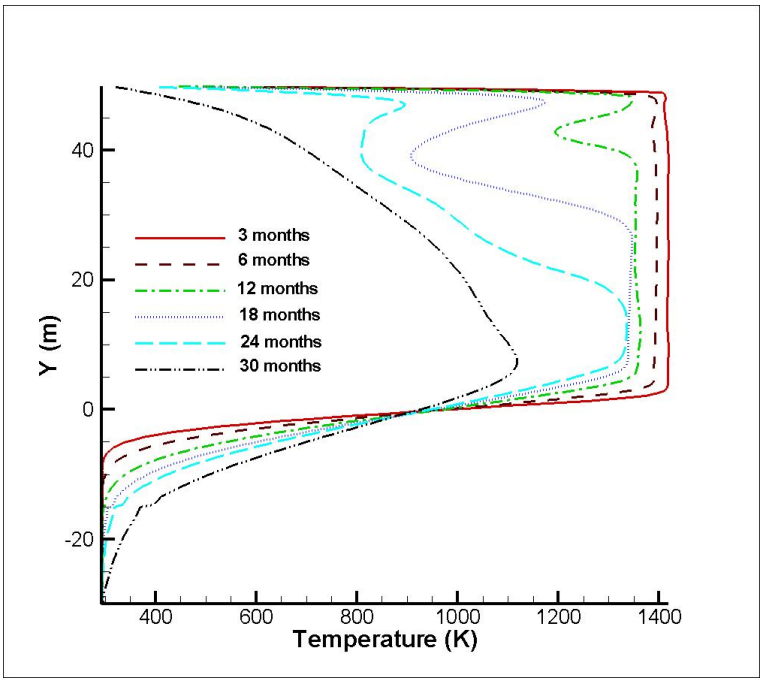

Figure 3-12(a). Variation of Internal Temperature Gradient for Lava Cooling: Simulations With Variable Thermal Conductivity, Variable Density, and Rain

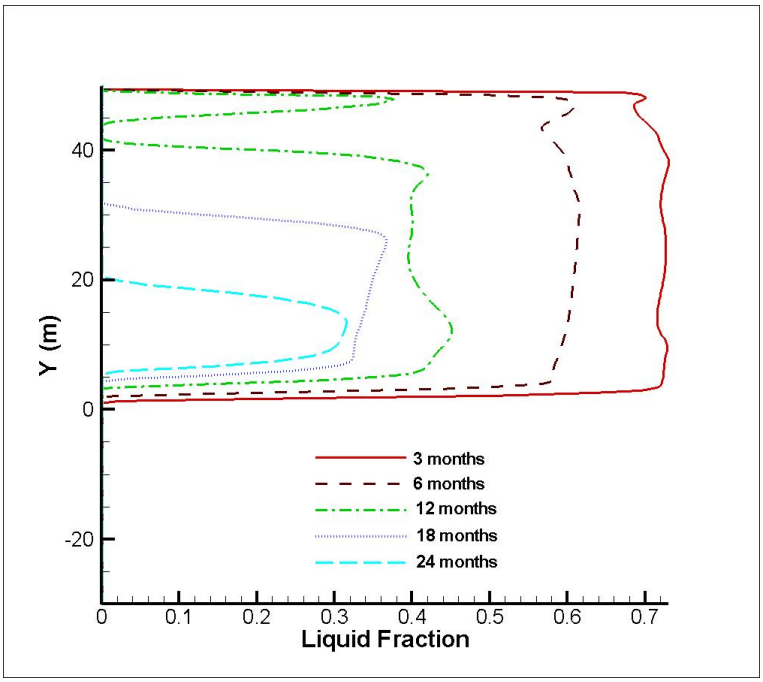

Figure 3-12(b). Variation of Liquid Fraction and Degree of Solidification for Lava Cooling: Simulations With Variable Thermal Conductivity, Variable Density, and Rain

variation of the liquid fraction. Figure 3-9(a) shows significant variation in the internal temperature gradient. As the numerical solution progresses over time, several inflection points can be seen in the temperature curve on the region of the hot lava core. Figure 3-9(b) shows the inflection points; these can also be attributed to the fact that the viscosity is assumed to be constant in the simulations, while the density is temperature dependent. Note that after 24 months, the liquid fraction has a maximum value of 0.35 over a small length of 21 m [70 ft]. This signifies that the majority of the hot lava core has solidified within 24 months.

Figure 3-10 shows the contours of temperature at various times obtained with variable thermal conductivity, variable density, and rain. The figures show that there is a plume-type structure in the temperature field and the reduction in the temperature in the core hot lava zone is significantly higher compared to the cases without rain. Including rain in the simulations with variable thermal conductivity and variable density results in a greater reduction of temperature (over a larger distance) in the hot lava zone compared to the simulations without rain.

Figure 3-11 shows the contours for the liquid fraction with rain. As can be observed, including rain results in faster solidification. Figure 3-12(a) shows the variation of internal temperature gradient for the simulations with rain. Figure 3-9(a) shows a significant temperature reduction after 24 months and 30 months compared to the temperatures observed in simulations with no rainfall. The effect of rainfall is only noticeable after 18 months. For the temperature profiles obtained at 24 months and 30 months, the peak temperature in the lava core region is significantly lower compared to the temperature obtained without rain. Figure 3-12(b) shows the corresponding variation of liquid fraction: after 24 months, most of the lava has solidified. However, the inclusion of heat loss due to rain does not influence the liquid fraction as much as it influences the internal temperature gradient. Overall, it can be concluded that variable thermal conductivity and variable density significantly influences the thermal field and the temperature. Note that the convection pattern observed in these cases may not be observed in reality. It may be an artifact of the computational method (constant viscosity along with temperature-dependent thermal conductivity and density). To evaluate the effect of these properties, additional simulations are carried out with all temperature-dependent properties.

3.3 Simulation Results With Variable Viscosity, Variable Thermal Conductivity, and Variable Density

Figures 3-13 through 3-16 show the results obtained from computations with variable thermal conductivity, variable viscosity formula (Costa and Macedenio, 2005), and variable density. As explained earlier, the variable properties are chosen to reflect the reality whereby these properties change as the lava cools. Modeling of rain is considered in the simulations. Figures 3-13 and 3-14 illustrate the temperature and liquid fraction for the present simulations. Figure 3-13 shows the contours of temperature at different time constants over a period of 30 months. A significant difference can be observed between these results and those obtained with constant thermal conductivity and density, as well as with results obtained using/applying variable thermal conductivity, variable density, and constant viscosity.

The plumelike structures that are present in the simulations with variable thermal conductivity, variable density, and constant viscosity are no longer observed in the current results. The change in viscosity with temperature may more realistically predict the thermal field. However, compared to the earlier results from runs using constant properties, crust development slows somewhat. There may be two reasons for this. First, the changing viscosity with temperature also influences the heat transfer, and as a result, the crust takes longer to develop. The temperature of the core is lower than that observed in the constant value case because a

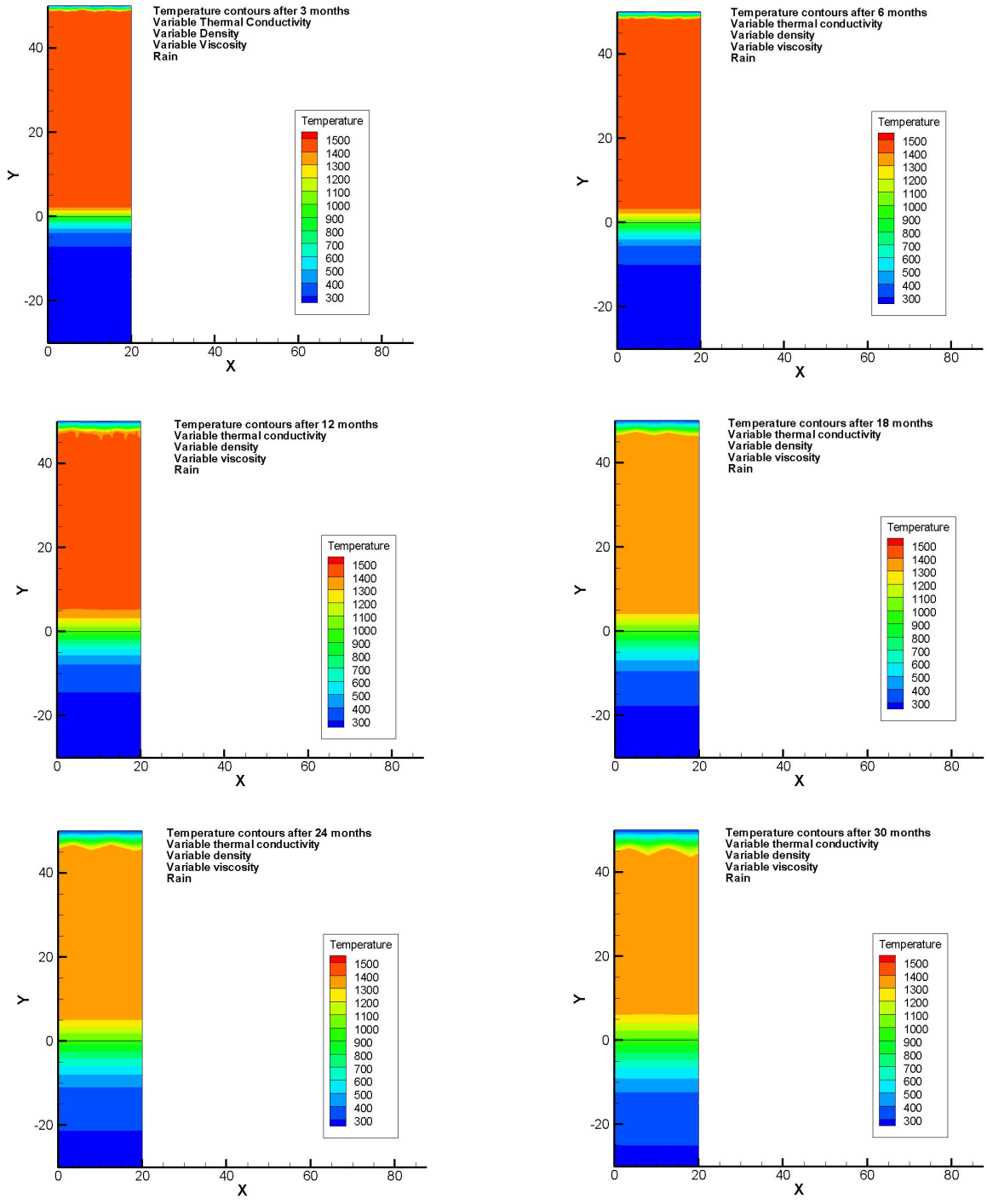

Figure 3-13. Contours of Static Temperature for Lava Cooling at Various Times: Simulations With Variable Thermal Conductivity, Variable Density, Variable Viscosity, and Rain

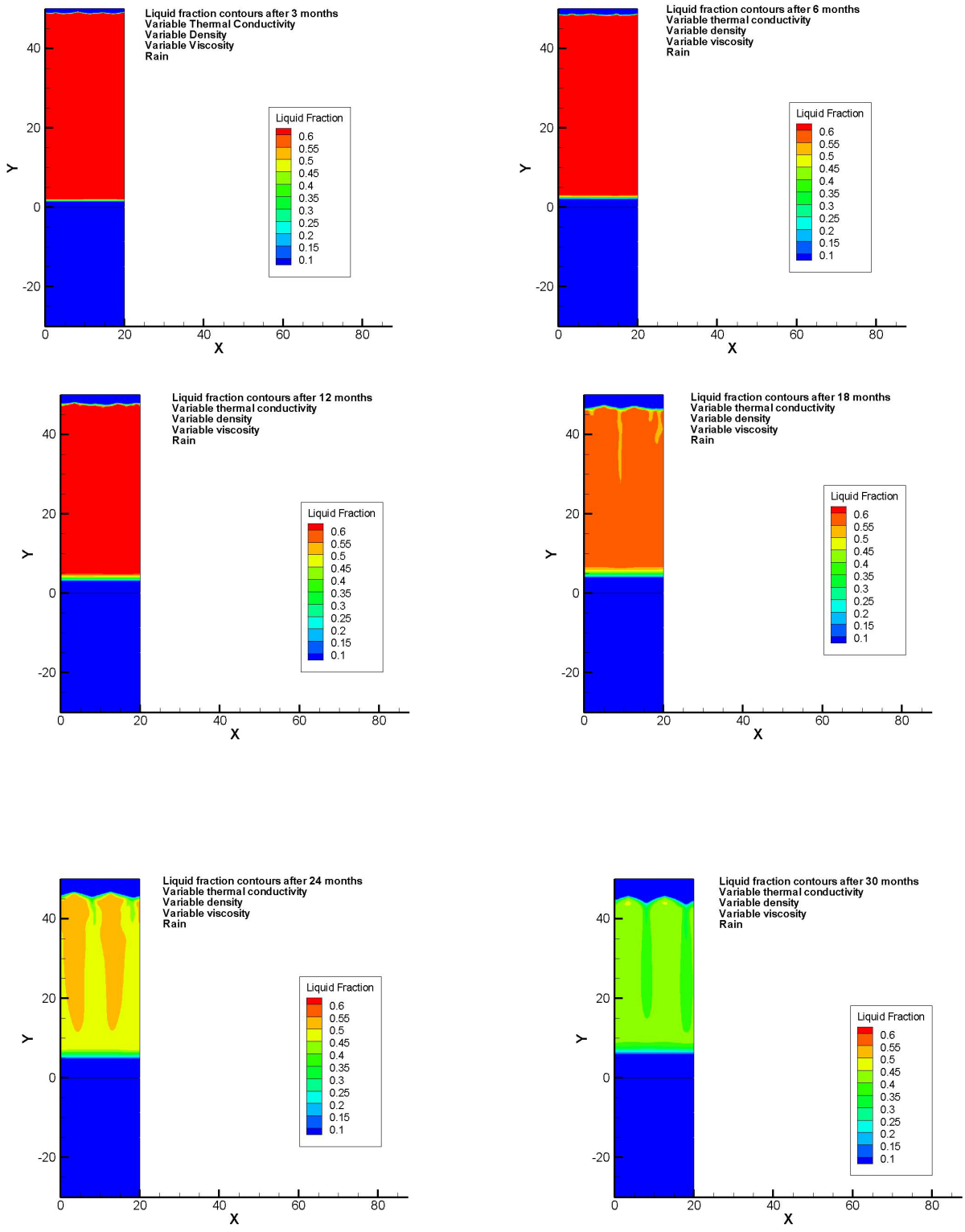

Figure 3.14. Contours of Liquid Fraction for Lava Cooling at Various Times: Simulations With Variable Thermal Conductivity, Variable Density, Variable Viscosity, and Rain

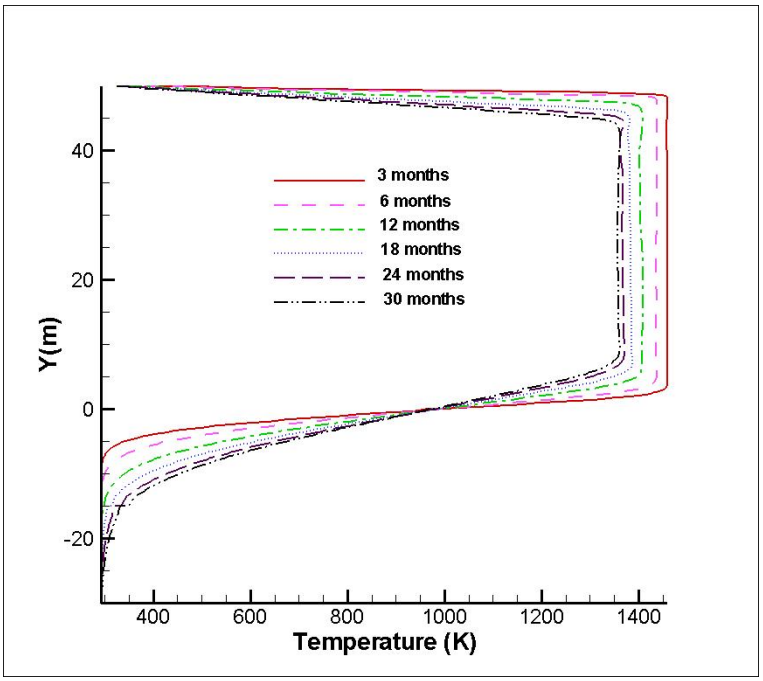

Figure 3-15. Variation of Internal Temperature Gradient for Lava Cooling: Simulations With Variable Thermal Conductivity, Variable Density, Variable Viscosity, and Rain

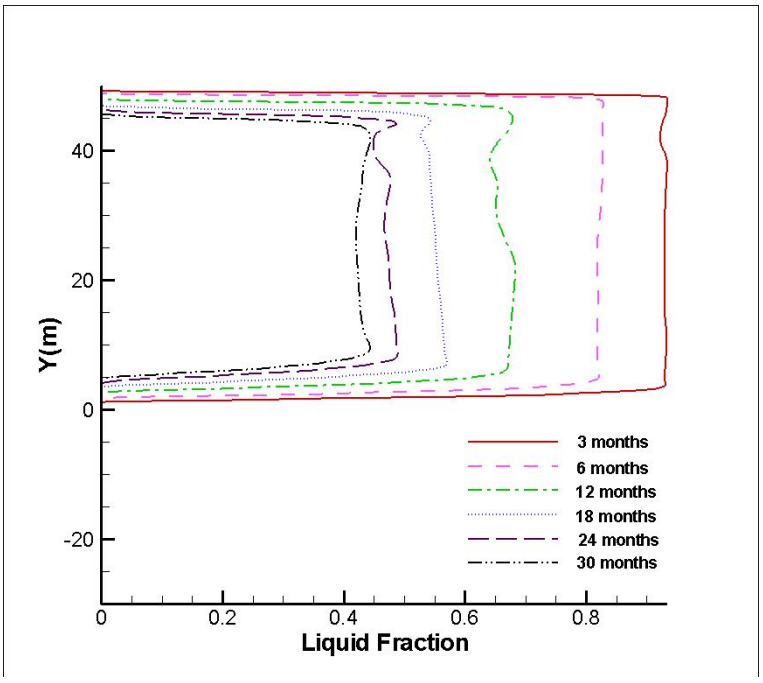

Figure 3-16. Variation of Liquid Fraction and Degree of Solidification for Lava Cooling: Simulations With Variable Thermal Conductivity, Variable Density, Variable Viscosity, and Rain

variable viscosity also alters the overall temperature and heat exchange between the different layers. As a result, the lava cools down slower than a constant viscosity case. Secondly, for this lava cooling simulation with variable viscosity, the upper limit of the temperature is 1,350 °K [1,970 °F]. In the earlier simulations, the temperature limit is 1,500 °K [2,240 °F]; thus, the larger difference in temperature between lava and atmosphere may have caused greater cooling in the earlier case.

Figure 3-14 shows the corresponding contours for the liquid fraction at various times for simulations with variable viscosity, variable thermal conductivity, and variable density. The figures at various times illustrate the rapid progress of the solidification front. After 30 months, a significant part of the entire hot lava core has solidified. Figure 3-14 also shows the formation of Rayleigh-Taylor instabilities. Lava cooling at the top generates small cooler plumes and thermal convection patterns that move downwards. Brandeis and Jaupart (1986) also observed formation of similar plumelike structures during magma body cooling in their experimental analysis. However note that Brandeis and Jaupart (1986) carried out the experiments with analog fluids. It is possible that the analog fluid may have produced these plumes, whereas magma may not produce these plumes in all real cases. However, the current fluid dynamics computations do show the formation of these plumes.

As magma (or lava) cools, its density increases and the probability of developing convective instability increases. However, at the same time, the magma also crystallizes and this crystallization also increases its viscosity as well as stabilizes against convective instability. The liquidus temperature influences both crystallization and convective instability. According to Brandeis and Jaupart (1986), as the temperature of the interior magma (or in our case, lava core) decreases toward the solidus, the system generates more plumes. However, note that the Brandeis and Jaupart (1986) analysis applied to cooling of the magma chamber, which is internal flow. The present analysis is for external cooling of lava, but similarities can be observed with the results Brandeis and Jaupart (1986) obtained. The formation of the plume like structure is only possible in variable viscosity fluids and is not observed in fluids with constant viscosities. This implies that the formation of the plume-like structure is a direct result of the complex interplay between temperature and viscosity. Also note that the current model does not include exclusive modeling of crystallization or changes in rheology, such as a liquid-viscoplastic transition. Viscosity also increases in the liquid as it cools and properties change to visco-elastic—the current work and these experiments (Brandeis and Jaupart, 1986) did not model this. Hence, it can also be inferred that the plumes might develop in real cooling lava, but they may be accentuated by the model experiment conditions.

In addition, for the case with constant viscosity, which is very low compared with the variable viscosity, the instability develops quickly. This means there is less time for heat transfer, so the density differences between the cooler part of the lava and the surrounding lava are larger. This in turn also speeds up the instability or the plume development. Hence, simulations with constant viscosity are extreme and unlikely to occur in nature. With variable viscosity, the high viscosity slows down the instability development, there is more time for heat transfer, and the density difference is small, further slowing the instability development. When the viscosity is very high, the process is very slow and there is enough time for heat transfer. The Rayleigh-Taylor instability only happens at a small scale, and the large-scale, plumelike structures never can develop as these simulation results show.

Figure 3-15 shows the variation of the internal temperature gradient and Figure 3-16 shows the variation of the liquid fraction in the simulations. The variation of the internal temperature gradient is very similar to that obtained from the baseline simulations shown in Figure 3-3(a).

One can observe that the temperature for the 30-m [98-ft]-thick portion of the lava core gradually changes as the core gets cooler. In a period of 30 months, the lava core temperature decreases by approximately 200 °K [360 °F]. The top and bottom layers of the lava core undergo significant changes in temperature and crust formation. The bottom layers of the hot lava core also undergo temperature changes at a faster rate with time than the top layers. Figure 3-16 shows that the liquid fraction decreases from 0.8 to 0.4 in 30 months, indicating that significant solidification of the lava core region has taken place. Comparing Figures 3-3(a), 3-9(a), and 3-15(a) reveals the significant influence of lava viscosity on the predicted temperature and lava cooling.

3.4 Baseline Simulation Results With Different Convective Heat Transfer Coefficient

Figures 3-17 and 3-18 show the effect of convective heat transfer coefficient on the variation of internal temperature gradient. The values chosen are 50 W/m^2K [8.8 BTU h^{-1} ft^{-2} $°F^{-1}$], 75 W/m^2K [13.2 BTU h^{-1} ft^{-2} $°F^{-1}$], and 100 W/m^2K [17.6 BTU h^{-1} ft^{-2} $°F^{-1}$]. While Figure 3-17 shows the variation of temperature after 18 months, Figure 3-18 shows the variation of temperature after 24 months. The results are obtained from simulations with constant thermal conductivity, constant density, and rain. Note that for increasing convective heat transfer coefficient, the temperature also decreases. A comparison of Figures 3-17 and 3-18 shows that the effect of convective heat transfer from the top boundary of the hot lava becomes more dominant at later times. The difference in temperatures obtained for the three values of convective heat transfer coefficient at 30 months is greater than the temperature difference obtained for the 3 values of convective heat transfer coefficient at 18 months.

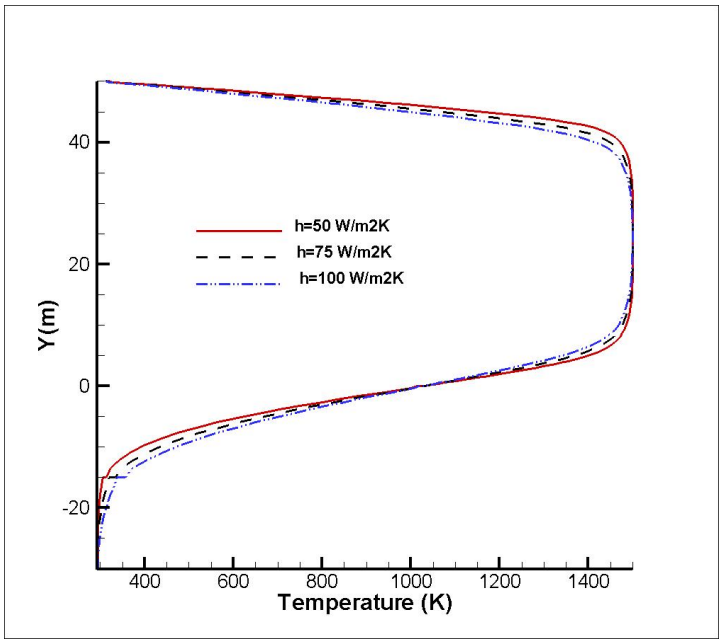

Figure 3-17. Variation of Internal Temperature Gradient for Lava Cooling After 18 Months: Effect of Convective Heat Transfer in Simulations With Constant Thermal Conductivity, Constant Density, and Rain

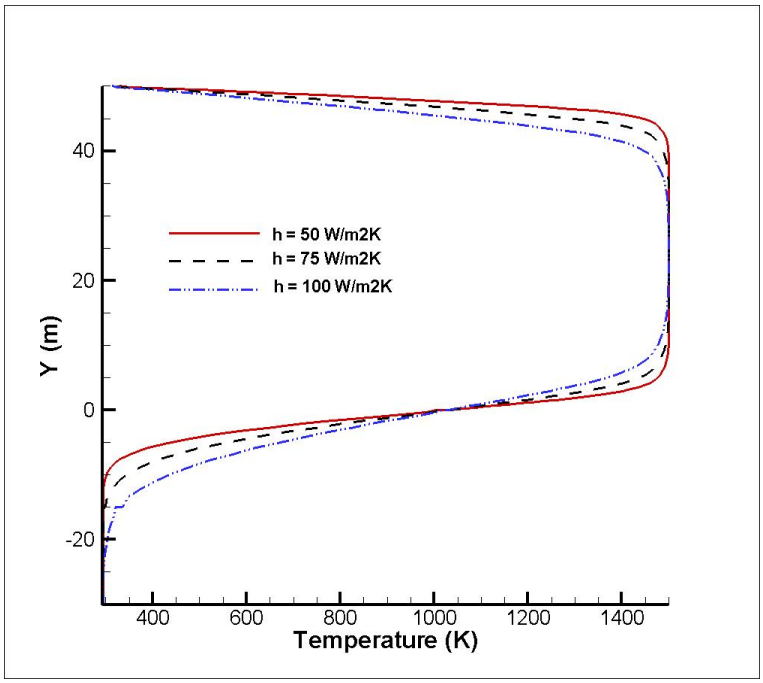

Figure 3-18. Variation of Internal Temperature Gradient for Lava Cooling After 30 Months: Effect of Convective Heat Transfer in Simulations With Constant Thermal Conductivity, Constant Density, and Rain

4 CONCLUSIONS

In the present work, computational modeling was conducted to investigate the cooling of hot bodies on the Earth's surface under different environmental conditions. For the present application, cooling of lava on the Earth's surface was considered. Numerical simulations provided critical insights into the long-term (~3 years) thermal behavior of hot bodies in contact with the ground (lava and rock substrate) under natural conditions.

Salient points of these analyses follow:

- Multimode heat transfer takes place from a hot body kept in the open atmosphere. From the top surface, the heat transfer is dominated by convection and radiation, whereas in the interface between the hot and cold bodies, heat transfer takes place through the conduction mode only.

- Treatment of lava viscosity significantly influences the degree of lava cooling. Simulations with variable thermal conductivity and variable density with constant viscosity resulted in an unphysical, plume-type structure within the hot lava core.

- The thermal field and solidification pattern varied significantly between simulations with a constant viscosity and those with a variable viscosity. Rayleigh-Taylor instabilities can be observed with variable properties (thermal conductivity, density and viscosity). Rayleigh-Taylor instability takes longer time to grow for more viscous fluid and smaller density difference.

- The inclusion of heat loss due to rain does not have any significant effect on the simulation results with constant thermal conductivity and constant density.

- The temperature of the substrate beneath the hot lava core increases in contact with the hot lava. The heat transfer between the hot lava and the substrate below it primarily takes place through conduction.

For simulations with variable properties and rain, the effect of rain on the cooling is not prominent during the initial time period (1 year). However, after a significant time (~2 years), the effect of rain is manifested through the lower values of the lava core temperature. This is thought to be a realistic measure of this natural effect on cooling of hot lava bodies. Higher values of convective heat transfer coefficient result in lower temperatures, and the effect is manifested in the later stages of cooling. The results presented in this report are preliminary and do not constitute a comprehensive analysis of atmospheric lava cooling. However, this analysis takes into account all modes of heat transfer in the computations. The current analysis simulated the cooling of a single lava lobe/sheet under realistic conditions of radiative and forced convective cooling. This analysis does not include the effect of daily atmospheric temperature variation on the predicted thermal field and temperature. However, the effect of daily atmospheric temperature variation is expected to be minimal (Kesthelyi and Denlinger, 1996). The temperature patterns inside the cooling lava body provide insight into the cooling and solidification history for basaltic lava in the open atmosphere with constant and variable properties.

5 REFERENCES

ANSYS, Inc. "ANSYS FLUENT Version 12.1, User's Guide." Canonsburg, Pennsylvania: ANSYS, Inc. 2009.

Brandeis, G. and C. Jaupart. "On the Interaction Between Convection and Crystallization in Cooling Magma Chambers." *Earth and Planetary Science Letters.* Vol. 77, Issues 3–4. pp. 345–361. 1986.

Costa, A. and G. Macedenio. "Numerical Simulation of Lava Flows Based on Depth-Averaged Equations." *Geophysical Research Letters.* Vol. 32. L05304, doi: 10.1029/2004GL021817. 2005.

Costa, A. and G. Macedenio. "Viscous Heating in Fluids with Temperature Dependent Viscosity: Implications for Magma Flows." *Nonlinear Processes in Geophysics.* Vol. 10. pp. 545–555. 2003.

Crisp, J. and S. Baloga. "A Model for Lava Flows With Two Thermal Components." *Journal of Geophysical Research.* Vol. 95. pp. 1,255–1,270. 1990.

Dragoni, M. "A Dynamical Model of Lava Flows Cooling by Radiation." *Bulletin of Volcanology*. Vol. 51. pp. 88–95. 1989.

Gresho, P.M., R.L. Lee, and R.L. Sani. "On the Time-Dependent Solution of the Incompressible Navier-Stokes Equations in Two and Three Dimensions." *Recent Advances in Numerical Methods in Fluids*. C. Taylor and K. Morgan, eds. Swansea, United Kingdom: Pineridge Press. 1980.

Head, J.W. and L. Wilson. "Volcanic Processes and Landforms on Venus: Theory, Predictions and Observations." *Journal of Geophysical Research*. Vol. 91. pp. 9,407–9,446. 1986.

Hon, K., J. Kauahikaua, R. Denlinger, and K. Mackay. "Emplacement and Inflation of Pahoehoe Sheet Flows: Observations and Measurements of Active Lava Flows on Kilauea Volcano, Hawaii." *Geological Society of America Bulletin*. Vol. 106. pp. 351–370. 1994.

Ishihara, K., M. Iguchi, and K. Kamo. "Numerical Simulation of Lava Flows on Some Volcanoes in Japan, in Lava Flows and Domes: Emplacement Mechanisms and Hazard Implications." J. H. Fink, ed. *IAVCEI Proceeding Volcanology*. Vol. 2. pp. 174–207. 1990.

Keszthelyi, L. "Calculated Effect of Vesicles on the Thermal Properties of Cooling Basaltic Lava Flows." *Journal of Volcanology and Geothermal Research*. Vol. 63, Issues 3–4. pp. 257–266. 1994.

Keszthelyi, L. and R. Denlinger. "The Initial Cooling of Pahoehoe Flow Lobes." *Bulletin of Volcanology*. Vol. 58. pp. 5–18. 1996.

Keszthelyi, L., A.J.L. Harris, and J. Dehn. "Observations of the Effect of Wind on the Cooling of Active Lava Flows." *Geophysical Research Letters*. Vol. 30, Article No. 1989. 2003.

Neri, A. "A Local Heat Transfer Analysis of Lava Cooling in the Atmosphere: Application to Thermal Diffusion-Dominated Lava Flows." *Journal of Volcanology and Geothermal Research*. Vol. 81. pp. 215–243. 1998.

Patrick, M.R., J. Dehn, and K. Dean. "Numerical Modeling of Lava Flow Cooling Applied to the 1997 Okmok Eruption: Approach and Analysis." *Journal of Geophysical Research.* Vol. 109. B03202, DOI: 10.1029/2003JB002537. 2004.

Peck, D.L., M.S. Hamilton, and H.R. Shaw. "Numerical Analysis of Lava Lake Cooling Models: Part II, Application to Alae Lava Lake, Hawaii." *American Journal of Science.* Vol. 277. pp. 415–437. 1977.

Shaw, H.R., M.S. Hamilton, and D.L. Peck. "Numerical Analysis of Lava Lake Cooling Models: Part I, Description of the Method." *American Journal of Science*. Vol. 277. pp. 384–414. 1977.

Touloukian, Y.S., W.R. Judd, and R.F. Roy (editors). *Physical Properties of Rocks and Minerals*. New York City, New York: Hemisphere. p. 548. 1989.

Van Doormal, J.P. and G.D. Raithby. "Enhancements of the SIMPLE Method for Predicting Incompressible Fluid Flows." *Numerical Heat Transfer*. Vol. 7. pp. 147–163. 1984.

Van Leer, B. "Toward the Ultimate Conservative Difference Scheme IV. A Second Order Sequel to Gudonov's Method." *Journal of Computational Physics*. Vol. 32. pp. 101–136. 1979.

Wooster, M.J., R. Wright, S. Blake, and D.A. Rothery. "Cooling Mechanisms and an Approximate Thermal Budget for the 1991–1993 Mount Etna Lava Flow." *Geophysical Research Letters*. Vol. 24. pp. 3,277–3,280. 1997.

Young, P. and G. Wadge. "FLOWFRONT: Simulation of a Lava Flow." *Computers and Geosciences.* Vol. 16. pp. 1,171–1,191. 1990.